Algebraic & Geometric Topology

Volume 26 (2026)

On homology concordance in contractible manifolds and two-bridge links

Hugo Zhou

Algebraic & Geometric Topology **26**:5 (2026) 1597–1634
DOI: 10.2140/agt.2026.26.1597
Published: May 29, 2026

On homology concordance in contractible manifolds and two-bridge links

HUGO ZHOU

Let $\widehat{\mathcal{C}}_{\mathbb{Z}}$ be the group which consists of manifold-knot pairs (Y, K) modulo homology concordance, where Y is an integer homology sphere bounding an integer homology ball, and let $\mathcal{C}_{\mathbb{Z}}$ be the subgroup consisting of pairs (S^3, K). Dai, Hom, Stoffregen and Truong showed that the quotient group $\widehat{\mathcal{C}}_{\mathbb{Z}}/\mathcal{C}_{\mathbb{Z}}$ admits a $\mathbb{Z}^\infty$-summand. In this paper, we improve the result by showing that there exists a family $\{(Y, K_m)\}_{m>1}$ generating a $\mathbb{Z}^\infty$-summand where Y is the boundary of a smooth contractible 4-manifold. In fact, we give a $\mathbb{Z}$-count of such families.

The examples are constructed using a family of knots obtained by blowing down a component of a two-bridge link. They are studied in Jonathan Hales's thesis. Using the algorithm due to Ozsváth, Szabó and Hales we give a classification of the knot Floer homology of a larger family of such knots that might be of independent interest.

1 Introduction

The integer homology concordance group $\widehat{\mathcal{C}}_{\mathbb{Z}}$ consists of pairs (Y, K) where Y is an integer homology sphere bounding an integer homology ball and K is a knot in Y, where the group operation is induced by the connected sum. Two classes (Y_1, K_1) and (Y_2, K_2) are equivalent if and only if there exists a pair $\partial(W, \Sigma) = (Y_1, K_1) \sqcup -(Y_2, K_2)$, where W is an integer homology cobordism and Σ a smoothly embedded cylinder in W. The subgroup $\mathcal{C}_{\mathbb{Z}}$ consists of pairs (S^3, K). A class (Y, K) is nonzero in $\widehat{\mathcal{C}}_{\mathbb{Z}}/\mathcal{C}_{\mathbb{Z}}$ if and only if K is not concordant to any knot in S^3 in any homology cobordism, or equivalently if and only if K does not bound any PL-disk in any homology ball with boundary Y.

The first nontrivial class $(Y, K) \in \widehat{\mathcal{C}}_{\mathbb{Z}}/\mathcal{C}_{\mathbb{Z}}$ was found by Levine [13], building on Akbulut's work [1]. Hom, Levine and Lidman [11] proved that $\widehat{\mathcal{C}}_{\mathbb{Z}}/\mathcal{C}_{\mathbb{Z}}$ is infinitely generated and admits a $\mathbb{Z}$-subgroup. Using the infinite family found in [20], Dai, Hom, Stoffregen and Truong [6] showed that $\widehat{\mathcal{C}}_{\mathbb{Z}}/\mathcal{C}_{\mathbb{Z}}$ admits a $\mathbb{Z}^\infty$-summand.

Among each infinite family of manifold-knot pairs which gives rise to the $\mathbb{Z}^\infty$-summand in the literature so far, the manifolds are always of the form $M_n \# -M_n$, such that they bound homology balls, but not necessarily smooth contractible manifolds. This paper strengthens the existing result by giving an infinite family of knots in the boundary of a smooth contractible manifold that generates a $\mathbb{Z}^\infty$-summand in $\widehat{\mathcal{C}}_{\mathbb{Z}}/\mathcal{C}_{\mathbb{Z}}$. In fact, we give a $\mathbb{Z}$-count of such families.

Imposing that the homology spheres bound smooth contractible manifolds guarantees that every knot in the boundary has trivial image in the fundamental group of the 4-manifold under the inclusion map.

MSC2020: 57K10, 57K18.

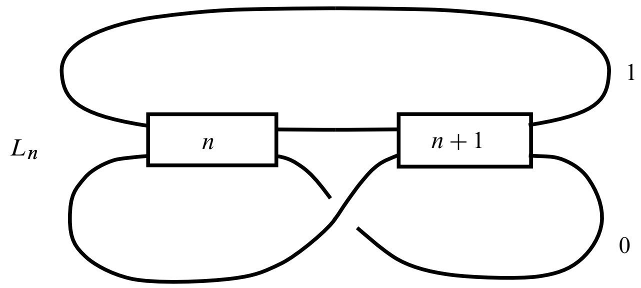

Figure 1: The two-bridge link L_n whose $(1,0)$-framed surgery yields the integer homology sphere Y_n that bounds a contractible manifold. The number in the box indicates the number of right-handed full-twists.

Therefore, there is no homotopic obstruction for the knots to bound PL-disks, making it a more interesting and more difficult question.

Consider the Mazur-type manifold Y_n with $n \geq 1$ (see [3]) as depicted in Figure 1, obtained from a $(1,0)$-framed surgery on a two-bridge link L_n. From a standard argument that switches the 0-framed two handle to a dotted circle, we see that Y_n bounds a contractible 4-manifold. (Both components of L_n are unknotted and they intersect algebraically once.) Let $K_n \subset S^3$ be the knot obtained from L_n by blowing down the $+1$-framed unknot component. It follows that $S^3_{-1}(K_n) = Y_n$ bounds a contractible 4-manifold.

Let $\mu^{(2n)}_{m,1}$ be the image of the $(m,1)$-cable of the meridian in the -1-surgery on K_{2n}.

Theorem 1.1 *The family $\{(Y_{2n}, \mu^{(2n)}_{m,1})\}_{n>0,m>1}$ generates a $\mathbb{Z}^{\mathbb{Z}\oplus\mathbb{Z}}$ summand in $\widehat{\mathcal{C}}_{\mathbb{Z}}/\mathcal{C}_{\mathbb{Z}}$. In particular, for each fixed $n>0$, $\{(Y_{2n}, \mu^{(2n)}_{m,1})\}_{m>1}$ generates a $\mathbb{Z}^{\mathbb{Z}}$ summand in $\widehat{\mathcal{C}}_{\mathbb{Z}}/\mathcal{C}_{\mathbb{Z}}$.*

As abelian groups, $\mathbb{Z}^{\mathbb{Z}\oplus\mathbb{Z}}$ is of course isomorphic to $\mathbb{Z}^{\mathbb{Z}}$. Here by a $\mathbb{Z}^{\mathbb{Z}\oplus\mathbb{Z}}$ summand we would like to emphasize the existence of a (natural) two-parameter family of linear independent, surjective homomorphisms from $\widehat{\mathcal{C}}_{\mathbb{Z}}/\mathcal{C}_{\mathbb{Z}}$ to $\mathbb{Z}$. In this case the two parameters are given by n and m. (See Lemma 2.6 for the homomorphisms.) Note that the $\mathbb{Z}^{\mathbb{Z}}$ summand in [11; 20] is generated by knots living in infinitely many different manifolds, while here each family of knots $\{\mu^{(2n)}_{m,1}\}_{m>1}$ lives in the same 3-manifold Y_{2n}, which is the boundary of a smooth contractible 4-manifold.

Theorem 1.1 is the direct consequence of the two following theorems. Denote by C_k the complex isomorphic to $\mathrm{CFK}^\infty(S^3, T_{2,2k+1})$. First, using the filtered mapping cone formula [21], and with the help of the concordance homomorphisms defined in [6], we show the following:

Theorem 1.2 *Suppose a family of knots $\{J_{2k}\}_{k>0}$ satisfies that $\mathrm{CFK}^\infty(S^3, J_{2k}) \cong C_{2k} \oplus A$, where $H_*(A)=0$. Then the family $\{(S^3_{-1}(J_{2k}), \mu^{(2k)}_{m,1})\}_{k>0,m>1}$ generates a $\mathbb{Z}^{\mathbb{Z}\oplus\mathbb{Z}}$ summand in $\widehat{\mathcal{C}}_{\mathbb{Z}}/\mathcal{C}_{\mathbb{Z}}$, where $\mu^{(2k)}_{m,1}$ is the image of the $(m,1)$-cable of the meridian in the -1-surgery on J_{2k}. In particular, for each fixed $k>0$, $\{(S^3_{-1}(J_{2k}), \mu^{(2k)}_{m,1})\}_{m>1}$ generates a $\mathbb{Z}^{\mathbb{Z}}$ summand in $\widehat{\mathcal{C}}_{\mathbb{Z}}/\mathcal{C}_{\mathbb{Z}}$.*

Next, the knot Floer complex of the knot family K_n can be explicitly computed as follows. Ozsváth and Szabó [16, Section 6.2] give a description for a genus-one doubly pointed Heegaard diagram of any knot that results from blowing down the ± 1-surgery on one component of a two-bridge link. The

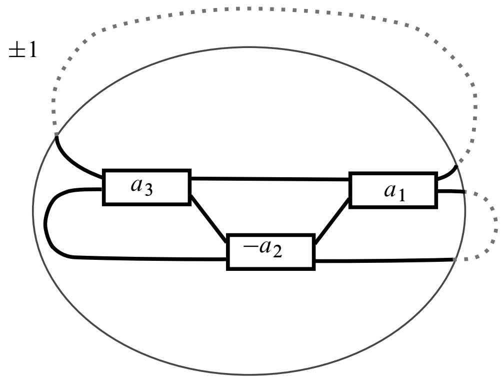

Figure 2: Blowing down one component of the closure of a rational tangle $[a_1, a_2, a_3]$ with a_1 and a_3 even yields the knot $K^{\pm}[a_1, a_2, a_3]$. The numbers in the boxes indicate the number of right-handed half-twists.

family of knots K_n is studied carefully in Jonathan Hales's thesis [8, Section 3]. Building on Ozsváth and Szabó's description, Hales develops a simple algorithm that outputs a $(1,1)$ diagram of all the knots that arise from blowing down the ± 1-surgery on one component of a two-bridge link. We review the details of this algorithm in Section 3. In particular, he proves the following theorem.

Theorem 1.3 [8] *For* $n > 0$, $\mathrm{CFK}^{\infty}(S^3, K_n) \cong C_n \oplus A$, *where* $H_*(A) = 0$.

See the $k = 1$ case of Proposition 4.27 for a more precise statement of Theorem 1.3. It is clear that Theorem 1.1 is the consequence of Theorems 1.2 and 1.3.

Remark 1.4 The family of knots K_n we consider here is the same family used to prove the infinite generation in [11], where the d-invariants of $1/p$ surgeries on $\mu_{1,1}^{(n)}$ are computed, using the fact that for certain p, the resulting manifolds are Brieskorn spheres. This is also similar to the approach employed in [2]. Interestingly, with the current computation we do not recover the infinite generation result with $\mu_{1,1}^{(n)}$ proved in [11], as it turns out that $\mathrm{CFK}^{\infty}(S^3_{-1}(K_n), \mu_{1,1}^{(n)})$ is locally equivalent to the trivial complex. In order to recover their result, one needs to in addition consider the nontrivial flip map over $\mathrm{CFK}^{\infty}(S^3_{-1}(K_n), \mu_{1,1}^{(n)})$.

1.1 Blowing down two-bridge links

We also explore the algorithm due to Ozsváth, Szabó and Hales. For a rational tangle $[a_1, \dots, a_\ell]$ whose closure is a two-component link, we can always arrange such that ℓ is odd and each a_i is even when i is odd. (See Lemma 3.2 and the discussion before that.) Denote by $K^{\pm}([a_1, \dots, a_\ell])$ the knot obtained from blowing down the ± 1-framed upper component. See Figure 2. It turns out that we can completely determine the knot Floer homology of $K^{\pm}([a_1, \dots, a_\ell])$ when $\ell \leq 3$. We include this classification result in the paper, with the expectation that these families of knots will generate more future applications.

The computation of the invariants has always been a main theme in Heegaard Floer homology. Despite significant development of the theory, there are still only a limited number of knot families whose knot

Floer complexes can be explicitly determined: L-space knots [17], thin knots [15; 18], $(1,1)$ almost L-space knots [4] (all determined by the Alexander polynomial) and certain cables of specific knots (using say [9], where the computations are already difficult).

Theorem 1.5 *The knot Floer complex of any knot $K^{\pm}([a_1,\dots,a_\ell])$ with $\ell = 1, 3$ and a_i even for odd i is classified, including Maslov gradings and filtration levels.*

The knot Floer chain homotopy types arise from our examples are novel. Consider the complexes D_s in Definition 4.20, the complexes $C_{n,k}$ in Definition 4.25 and the complexes $C'_{n,k}$ in Definition 4.30. Recall $C_n \cong \mathrm{CFK}^\infty(S^3, T_{2,2n+1})$ and let C_0 be the complex generated by a single element. We will show that the knot Floer complexes of various knots $K^{\pm}[n,1,n+k]$ with $n > 0$ and $k \geq 0$ consists of direct summands of the above complexes. (For detailed statements, see Propositions 4.27 and 4.31.) As mentioned earlier, the case for K^+ when $k = 1$ has already been done by Jonathan Hales. We include it into a framework suitable for a slightly larger family.

Moreover, this classification involves interesting techniques. For a general sequence $[a_1, b, a_3]$, we observe that changing b by 2 amounts to performing a full Dehn-twist around two basepoints. Concretely, if we let γ be an arc between the two base points, the Dehn-twist is performed along the closed loop $\gamma \cup_{S^0} \overline{\gamma}$, where $\overline{\gamma}$ is a copy of γ with the reversed orientation. See Figure 7 on page 1614. This is a local transformation in a neighborhood of γ, so we can opt to perform it in the very end. It turns out that each full Dehn-twist amounts to adding a box summand at the "closest" generator near γ. See Figure 8 on page 1616 for the effect on CFK^∞ and see Definition 4.8 for a precise definition of the "closest" generator. It follows that in order to recover any general sequence $[a_1, b, a_3]$, we need only consider the case $b = \pm 1$ and 0 with a *marked basis*. See Proposition 4.11 for more details.

This method allows us to reduce the full classification to a handful of cases. For instance, in Section 4.3 we will utilize it to show that the knot Floer complex corresponding to the sequence $[a_1, b, a_3]$ when b is even is isomorphic to $\mathrm{CFK}^\infty(S^3, T_{n,n+1})$ for certain n with a certain number of box summands added to some marked generators.

Remark 1.6 When $\ell > 3$, even though a closed formula seems unlikely, using similar methods as in this paper it is still very much feasible to determine the full knot Floer complex for singular examples of $K^{\pm}([a_1,\dots,a_\ell])$. Moreover, if one opts to compute partial invariants such as the local equivalence class or the τ invariant, then I believe the computation should be practical for a larger family of knots, and I expect the result to be interesting as well.

Organization

We perform the filtered mapping cone computations and prove Theorem 1.2 in Section 2. We review the algorithm by Ozsváth, Szabó and Hales in Section 3 and prove our classification result in Section 4. More detailedly, in Section 4.1, we prove the length-one case; in Section 4.2, we discuss the length-three case in general and prove some helpful lemmas; in Sections 4.3 through 4.7, we deal with the remaining cases with length-three.

2 Knot Floer homology of the cables of the knot meridian

In this section we prove Theorem 1.2. We will make use of the concordance invariants $\varphi_{i,j}$ defined in [5]. We refer the reader to the original paper for the detailed definitions. See [5, Section 3.2] for a worked out example. See [21, Example 8.1] for yet another example. Since $\varphi_{i,j}$ factors through the group of knotlike complexes over local equivalence [5, Proposition 4.42], instead of considering -1-surgery on the knot J_{2k} with $\mathrm{CFK}^\infty(S^3, J_{2k}) \cong \mathrm{CFK}^\infty(S^3, T_{4k+1}) \oplus A$, where $H_*(A) = 0$, it suffices to consider the -1-surgery on T_{4k+1}.

Theorem 1.2 follows from a computational result, Proposition 2.5. The computational tool is the filtered mapping cone formula [21], which combines [10; 19] to give a description of the knot Floer complex of the $(m,1)$-cable of the meridian in the image of a surgery along a knot. We include a brief review of this filtered mapping cone formula in the following subsection.

2.1 Preliminaries on the filtered mapping cone formula

Let $K \subset S^3$ be a knot with genus equal to g. For a given positive integer m, let $\mu_{m,1}$ denote the $(m,1)$-cable of the meridian of K in the -1-surgery on K. According to [21, Theorem 1.9], the knot Floer complex $\mathrm{CFK}^\infty(S^3_{-1}(K), \mu_{m,1})$ is filtered chain homotopy equivalent to the doubly filtered chain complex $X^\infty_m(K)$, defined to be the mapping cone of

$$\bigoplus_{s=-g+1}^{g+m-1} A_s^\infty \xrightarrow{v_s^\infty + h_s^\infty} \bigoplus_{s=-g}^{g+m-1} B_s^\infty, \tag{1}$$

where each A_s^∞ and B_s^∞ are isomorphic to $\mathrm{CFK}^\infty(S^3, K)$. The map $v_s^\infty : A_s \to B_s$ is the identity and the map $h_s^\infty : A_s \to B_{s-1}$ is the reflection along $i = j$ precomposed with U^s. Note that in general h_s^∞ is a graded filtered chain homotopy equivalence with respect to j-filtration on the domain and i-filtration on the range. For knots in S^3, since $\mathrm{HF}^-(S^3)$ is one-dimensional, h_s^∞ is unique up to filtered chain homotopy equivalence and therefore we may take it to be the reflection map. See [10, Lemma 2.18].

Let $\mathcal{I}$ and $\mathcal{J}$ be the double filtrations on the filtered mapping cone complex $X^\infty_m(K)$. We have for $[\boldsymbol{x}, i, j] \in A_s$,

$$\mathcal{I}([\boldsymbol{x}, i, j]) = \max\{i, j - s\}, \tag{2}$$

$$\mathcal{J}([\boldsymbol{x}, i, j]) = \max\{i - m, j - s\} - ms + \tfrac{1}{2}m(m+1), \tag{3}$$

and for $[\boldsymbol{x}, i, j] \in B_s$,

$$\mathcal{I}([\boldsymbol{x}, i, j]) = i, \tag{4}$$

$$\mathcal{J}([\boldsymbol{x}, i, j]) = i - m - ms + \tfrac{1}{2}m(m+1). \tag{5}$$

It is straightforward to check that for $s < -g + 1$, the map h_s induces an isomorphism on the homology; for $s > g + m - 1$, the map $v_s(K)$ induces an isomorphism on the homology, which justifies the truncation of the mapping cone.

The general strategy for computation involves finding a *reduced* basis for $X_m^\infty(K)$, where every term in the differential strictly lowers at least one of the filtrations. This can be achieved through a cancellation process (see, for example, [14, Proposition 11.57]) as follows: Suppose $\partial x_i = y_i +$ lower filtration terms, where the double filtration of y_i is the same as x_i. Then the subcomplex of $X_m^\infty(K)$ generated by all such $\{x_i, \partial x_i\}$ is acyclic, and $X_m^\infty(K)$ quotient by this complex is reduced. Alternatively, one can view the above process as a change of basis that splits off acyclic summands which individually lie entirely in one double-filtration level.

2.2 Computation

Recall that it suffices to consider the $(m,1)$-cable of the knot meridian in the -1-surgery on T_{4k+1}. For $k \geq 1$, the complex $C_{2k} = \mathrm{CFK}^\infty(S^3, T_{2,4k+1})$ is generated by a_i for $i = 1, \dots, 2k$ with coordinate $(0, -2k+2i-1)$ and b_i for $i = 1, \dots, 2k+1$ with coordinate $(0, -2k+2i-2)$. The Maslov grading is supported in b_{2k+1} and the differentials are given by

$$\partial a_i = U b_{i+1} + b_i \quad \text{for } i = 1, \dots, 2k.$$

Via the isomorphism with $\mathrm{CFK}^\infty(S^3, T_{2,4k+1})$, denote the generators in A_s by $a_i^{(s)}$ for $i = 1, \dots, 2k$ and $b_i^{(s)}$ for $i = 1, \dots, 2k+1$ and the generators in B_s by $a_i'^{(s)}$ and $b_i'^{(s)}$, where $s = -2k+1, \dots, 2k+m-1$. The differential on the mapping cone is given by

$$\begin{aligned}
\partial a_i^{(s)} &= b_i^{(s)} + U b_{i+1}^{(s)} + a_i'^{(s)} + U^{s+2k+1-2i}(a_{2k-i+1}'^{(s-1)}),\\
\partial b_i^{(s)} &= b_i'^{(s)} + U^{s+2k+2-2i}(b_{2k-i+2}'^{(s-1)}),\\
\partial a_i'^{(s)} &= b_i'^{(s)} + U b_{i+1}'^{(s)}.
\end{aligned}$$

We first look to choose a reduced basis for the complex of $X_m^\infty(T_{2,4k+1})$. As a subcomplex of $X_m^\infty(T_{2,4k+1})$, each B_s is one dimensional. Indeed, quotienting out $\{a_i'^{(s)}, \partial a_i'^{(s)}\}_{1\leq i\leq 2k}$ leaves us with the sole generator $b_{2k+1}'^{(s)}$; define $\beta_s = b_{2k+1}'^{(s)}$ after the change of basis.

Next, for the complex A_s, observe that $a_i^{(s)}$ and $U b_{i+1}^{(s)}$ are in the same coordinate if $-2k+2i-1 \geq s$, and similarly $a_i^{(s)}$ and $b_i^{(s)}$ are in the same coordinate if $-2k+2i-1 \leq s-m$. So we may quotient out $\{a_i^{(s)}, \partial a_i^{(s)}\}$ for $i \geq k + \frac{s+1}{2}$ and $i \leq k + \frac{s-m+1}{2}$. We have obtained a reduced model of $X_m^\infty(T_{2,4k+1})$. As a notational shorthand, let us define

$$f(m,s) = \frac{m(m+1)}{2} - ms, \quad i_{m,s}^{(t)} = \min\left\{k + \left\lceil \frac{s-1}{2} \right\rceil, 2k\right\}, \quad i_{m,s}^{(b)} = \max\left\{k + 1 + \left\lceil \frac{s-m}{2} \right\rceil, 1\right\}$$

such that in the reduced model each complex A_s is generated by $a_i^{(s)}$ with $i_{m,s}^{(b)} \leq i \leq i_{m,s}^{(t)}$ and $b_i^{(s)}$ with $i_{m,s}^{(b)} \leq i \leq i_{m,s}^{(t)} + 1$. The induced differentials on the chain complex are

$$\partial a_i^{(s)} = b_i^{(s)} + U b_{i+1}^{(s)}, \tag{6}$$

$$\partial b_i^{(s)} = U^{2k+1-i}\beta_s + U^{2k+1-i+s}\beta_{s-1}, \tag{7}$$

and the filtration level of the generators are

$$\mathcal{J}(a_i^{(s)}) = f(m,s) - 2k - s - 1 + 2i, \tag{8}$$

$$\mathcal{J}(b_i^{(s)}) = f(m,s) - 2k - s - 2 + 2i, \tag{9}$$

$$\mathcal{J}(\beta_s) = f(m,s+1), \tag{10}$$

$$\mathcal{I}(a_i^{(s)}) = \mathcal{I}(b_i^{(s)}) = \mathcal{I}(\beta_s) = 0 \tag{11}$$

for $-2k+1 \le s \le 2k+m-1$ and suitable i as discussed above. For the purpose of computing concordance invariants, we will show the mapping cone can be further truncated. Let

$$X_m^\infty(T_{2,4k+1})\langle \ell \rangle = \bigoplus_{s=-\ell+m}^{\ell} A_s^\infty \xrightarrow{v_s^\infty + h_s^\infty} \bigoplus_{s=-\ell+m-1}^{\ell} B_s^\infty.$$

Note that under this notation $X_m^\infty(T_{2,4k+1}) = X_m^\infty(T_{2,4k+1})\langle 2k+m-1\rangle$.

Lemma 2.1 *For any $k \ge 1$ and $m \ge 2$, the filtered complex $X_m^\infty(T_{2,4k+1})\langle 2k+m-1\rangle$ is isomorphic to $X_n^\infty(T_{2,4k+1})\langle m-1\rangle \oplus D$ up to a filtered change of basis, where $H_*(D) = 0$.*

Proof We will show that for $m \le \ell \le 2k+m-1$, the complex $X_m^\infty(T_{2,4k+1})\langle \ell\rangle$ is isomorphic to $X_m^\infty(T_{2,4k+1})\langle \ell-1\rangle \oplus D'$ up to a change of basis, where $H_*(D') = 0$. For every such ℓ, in $X_m^\infty(T_{2,4k+1})\langle \ell\rangle$ perform a change of basis

$$\beta_{-\ell+m-1} \mapsto \beta_{-\ell+m-1} + U^{\ell-m}\beta_{-\ell+m}, \quad \beta_\ell \mapsto \beta_\ell + U^\ell \beta_{\ell-1}.$$

By (7), as a result the complexes given by

$$A_{-\ell+m}^\infty \xrightarrow{h_{-\ell+m}} B_{-\ell+m-1}^\infty, \quad A_\ell^\infty \xrightarrow{v_\ell} B_\ell^\infty$$

both become summands under the new basis. The change of basis is clearly filtered with respect to the $\mathcal{I}$–filtration. For the $\mathcal{J}$–filtration, we compute

$$\begin{aligned}\mathcal{J}(\beta_{-\ell+m-1}) - \mathcal{J}(U^{\ell-m}\beta_{-\ell+m}) &= \mathcal{J}(\beta_{-\ell+m-1}) - (\mathcal{J}(\beta_{-\ell+m}) - \ell + m)\\ &= f(m,-\ell+m) - f(m,-\ell+m+1) + \ell - m = \ell \ge 0,\\ \mathcal{J}(\beta_\ell) - \mathcal{J}(U^\ell \beta_{\ell-1}) = \mathcal{J}(\beta_\ell) - &\mathcal{J}(\beta_{\ell-1}) + \ell = f(m,\ell+1) - f(m,\ell) + \ell = \ell - m \ge 0.\end{aligned}$$

Therefore the change of basis is filtered. □

We also record the filtration shift between the generators in the complex.

Definition 2.2 Suppose $U^c y$ is a nontrivial term in ∂x, where c is some constant and x, y are both generators. Define

$$\Delta_{\mathcal{I},\mathcal{J}}(x,y) = (\mathcal{I},\mathcal{J})(x) - (\mathcal{I},\mathcal{J})(U^c y)$$

and similarly define $\Delta_{\mathcal{I}}$ and $\Delta_{\mathcal{J}}$.

Clearly, $\Delta_{\mathcal{I},\mathcal{J}}(a_i^{(s)}, b_i^{(s)}) = (0,1)$ and $\Delta_{\mathcal{I},\mathcal{J}}(a_i^{(s)}, b_{i+1}^{(s)}) = (1,0)$ for each $i_{m,s}^{(b)} \le i \le i_{m,s}^{(t)}$. We also have:

Lemma 2.3 *For $-2k+1 \leq s \leq 2k+m-1$ and $i^{(b)}_{m,s} \leq i \leq i^{(t)}_{m,s}+1$,*

$$\Delta_{\mathcal{I},\mathcal{J}}(b_i^{(s)}, \beta_{s-1}) = (2k+1-i+s, i-1), \tag{12}$$

$$\Delta_{\mathcal{I},\mathcal{J}}(b_i^{(s)}, \beta_{s}) = (2k+1-i, m-s+i-1). \tag{13}$$

Proof By (7), (9), (10) and (11), we compute

$$\begin{aligned}
\Delta_{\mathcal{I},\mathcal{J}}(b_i^{(s)}, \beta_{s-1}) &= (\mathcal{I},\mathcal{J})(b_i^{(s)}) - (\mathcal{I},\mathcal{J})(U^{2k+1-i+s}\beta_{s-1}) \\
&= (0, f(m,s)-2k-s-2+2i) - (0, f(m,s)) + (2k+1-i+s, 2k+1-i+s) \\
&= (2k+1-i+s, i-1), \\
\Delta_{\mathcal{I},\mathcal{J}}(b_i^{(s)}, \beta_{s}) &= (\mathcal{I},\mathcal{J})(b_i^{(s)}) - (\mathcal{I},\mathcal{J})(U^{2k+1-i}\beta_{s}) \\
&= (0, f(m,s)-2k-s-2+2i) - (0, f(m,s+1)) + (2k+1-i, 2k+1-i) \\
&= (2k+1-i, m-s+i-1).
\end{aligned}$$

□

We have all the ingredients to calculate the concordance invariants $\varphi_{i,j}$. This will be done in two steps. First, we translate the complex $X_n^\infty(T_{2,4k+1})\langle m-1\rangle$ into the ring $\mathbb{F}[U,V]$. Then we further translate it into the ring $\mathbb{X}$ and perform a change of basis, resulting a standard complex, from which the invariants $\varphi_{i,j}$ can be readily read off.

Lemma 2.4 *Over the ring $\mathbb{F}[U,V]$, the complex $X_n^\infty(T_{2,4k+1})\langle m-1\rangle$ is generated by*

$$\{\beta_s \mid 0 \leq s \leq m-1\} \cup \{a_i^{(s)} \mid 1 \leq s \leq m-1,\ i^{(b)}_{m,s} \leq i \leq i^{(t)}_{m,s}\} \cup \{b_i^{(s)} \mid 1 \leq s \leq m-1,\ i^{(b)}_{m,s} \leq i \leq i^{(t)}_{m,s}+1\}$$

with differentials

$$\partial a_i^{(s)} = U b_{i+1}^{(s)} + V b_i^{(s)}, \tag{14}$$

$$\partial b_i^{(s)} = U^{\Delta_{\mathcal{I}}(b_i^{(s)},\beta_{s-1})} V^{\Delta_{\mathcal{J}}(b_i^{(s)},\beta_{s-1})} \beta_{s-1} + U^{\Delta_{\mathcal{I}}(b_i^{(s)},\beta_{s})} V^{\Delta_{\mathcal{J}}(b_i^{(s)},\beta_{s})} \beta_{s}. \tag{15}$$

Proof This follows trivially from (6), (7) and the definition of $\Delta_{\mathcal{I}}$ and $\Delta_{\mathcal{J}}$. □

We are ready to prove the following proposition. Compare with [21, Proposition 1.2].

Proposition 2.5 *We have*

$$\varphi_{i,j}(X_n^\infty(T_{2,4k+1})\langle m-1\rangle) = \begin{cases} -\sum_1^{s-1}(i^{(t)}_{m,s} - i^{(b)}_{m,s}+1) & \text{if } (i,j) = (1,0), \\ 1 & \text{if } (i,j) \in \{\Delta_{k,m}(s) \mid 1 \leq s \leq m-1\}, \\ 0 & \text{otherwise,} \end{cases}$$

where $\Delta_{k,m}(s)$ is given by

$$\Delta_{k,m}(s) = \begin{cases} \left(k - \left\lceil \frac{s-1}{2} \right\rceil, m+k-\left\lfloor \frac{s+1}{2} \right\rfloor\right) & s \leq 2k, \\ (0, 2k+m-s) & s \geq 2k. \end{cases}$$

Proof Continuing from Lemma 2.4, we can further translate the complex $X_n^\infty(T_{2,4k+1})\langle m-1\rangle$ into the ring

$$\mathbb{X} = \frac{\mathbb{F}[U_B, \{W_{B,i}\}_{i\in\mathbb{Z}}, V_T, \{W_{T,i}\}_{i\in\mathbb{Z}}]}{(U_B V_T, U_B W_{B,i} - W_{B,i+1}, V_T W_{T,i} - W_{T,i+1})}$$

using the maps

$$U \mapsto U_B + W_{T,0}, \quad V \mapsto V_T + W_{B,0}.$$

The differentials now reads

$$\begin{aligned}
\partial a_i^{(s)} &= (U_B + W_{T,0}) b_{i+1}^{(s)} + (W_{B,0} + V_T) b_i^{(s)}, \\
\partial b_i^{(s)} &= (U_B^{\Delta_\mathcal{I}(b_i^{(s)},\beta_{s-1})} W_{B,0}^{\Delta_\mathcal{J}(b_i^{(s)},\beta_{s-1})} + V_T^{\Delta_\mathcal{J}(b_i^{(s)},\beta_{s-1})} W_{B,0}^{\Delta_\mathcal{I}(b_i^{(s)},\beta_{s-1})})\beta_{s-1} \\
&\qquad + (U_B^{\Delta_\mathcal{I}(b_i^{(s)},\beta_s)} W_{B,0}^{\Delta_\mathcal{J}(b_i^{(s)},\beta_s)} + V_T^{\Delta_\mathcal{J}(b_i^{(s)},\beta_s)} W_{T,0}^{\Delta_\mathcal{I}(b_i^{(s)},\beta_s)})\beta_s.
\end{aligned}$$

Note that each term in the previous coefficient in $\mathbb{F}[U,V]$ becomes two terms in the above expression, one in the ideal (U_B) and one in the ideal (V_T). We perform the change of basis

$$\tilde{b}_i^{(s)} = \begin{cases} b_i^{(s)} + U_B^{-1} W_{B,0}(b_{i-1}^{(s)}) & \text{if } i = i_{m,s}^{(t)}+1, \\ b_i^{(s)} + U_B^{-1} W_{B,0}(b_{i-1}^{(s)}) + V_T^{-1} W_{T,0}(b_{i+1}^{(s)}) & \text{if } i_{m,s}^{(b)} < i < i_{m,s}^{(t)}+1, \\ b_i^{(s)} + V_T^{-1} W_{T,0}(b_{i+1}^{(s)}) & \text{if } i = i_{m,s}^{(b)}, \end{cases} \tag{16}$$

$$\tilde{\beta}_s = \begin{cases} \beta_s + V_T^{-s} W_{T,0}^{m-s} \beta_{s-1} & \text{if } s = 0, \\ \beta_s + V_T^{-s} W_{T,0}^{m-s} \beta_{s-1} + U_B^{s-m} W_{B,0}^{s} \beta_{s+1} & \text{if } 1 \le s \le m-2, \\ \beta_s + U_B^{s-m} W_{B,0}^{s} \beta_{s+1} & \text{if } s = m-1, \end{cases} \tag{17}$$

which simplifies the differentials to

$$\partial a_i^{(s)} = U_B \tilde{b}_{i+1}^{(s)} + V_T \tilde{b}_i^{(s)}, \tag{18}$$

$$\partial \tilde{b}_i^{(s)} = \begin{cases} V_T^{\Delta_\mathcal{J}(b_i^{(s)},\beta_s)} W_{T,0}^{\Delta_\mathcal{I}(b_i^{(s)},\beta_s)} \tilde{\beta}_s & \text{if } i = i_{m,s}^{(t)}+1, \\ U_B^{\Delta_\mathcal{I}(b_i^{(s)},\beta_{s-1})} W_{B,0}^{\Delta_\mathcal{J}(b_i^{(s)},\beta_{s-1})} \tilde{\beta}_{s-1} & \text{if } i = i_{m,s}^{(b)}, \\ 0 & \text{otherwise.} \end{cases} \tag{19}$$

Note that $\Delta_{\mathcal{I},\mathcal{J}}(b_i^{(s)}, \beta_{s-1}) - \Delta_{\mathcal{I},\mathcal{J}}(b_i^{(s)}, \beta_s) = (s, s-m)$ by (12) and (13) which justifies the change of basis (17). We have obtained a standard complex [5, Definition 5.1], where the sequence of vector length of each V-edges (starting from $\tilde{\beta}_0$) is

$$(\underbrace{\overbrace{-(1,0),\dots,-(1,0)}^{(i_{m,s}^{(t)}-i_{m,s}^{(b)}+1)\text{ copies}}, \Delta_{\mathcal{I},\mathcal{J}}(b_{i_{m,s}^{(t)}+1}^{(s)}, \beta_s)}_{1\le s\le m-1}, \dots).$$

To finish the proof, it suffices to show $\Delta_{k,m}(s) = \Delta_{\mathcal{I},\mathcal{J}}(b^{(s)}_{i^{(t)}_{m,s}+1}, \beta_s)$ for $1 \le s \le m-1$. Recall that $i^{(t)}_{m,s} = \min\{k + \lceil \frac{s-1}{2} \rceil, 2k\}$. Therefore

$$i^{(t)}_{m,s} + 1 = \begin{cases} k + \lceil \frac{s+1}{2} \rceil & \text{if } s \le 2k, \\ 2k+1 & \text{if } s \ge 2k. \end{cases}$$

By (13), we compute

$$\begin{aligned} \Delta_{\mathcal{I},\mathcal{J}}(b^{(s)}_{i^{(t)}_{m,s}+1}, \beta_s) &= \left(2k+1-k-\left\lceil \frac{s+1}{2} \right\rceil, m-s+k+\left\lceil \frac{s+1}{2} \right\rceil - 1\right) \\ &= \left(k - \left\lceil \frac{s-1}{2} \right\rceil, m+k-\left\lfloor \frac{s+1}{2} \right\rfloor\right) \quad \text{if } s \le 2k; \\ \Delta_{\mathcal{I},\mathcal{J}}(b^{(s)}_{i^{(t)}_{m,s}+1}, \beta_s) &= (2k+1-(2k+1), m-s+2k+1-1) \\ &= (0, 2k+m-s) \quad \text{if } s \ge 2k. \end{aligned}$$

□

Lemma 2.6 *Suppose* $\mathrm{CFK}^\infty(S^3, J_{2k}) \cong \mathrm{CFK}^\infty(S^3, T_{4k+1}) \oplus A$ *for* $k > 0$, *where* $H_*(A) = 0$. *Let* $\mu^{(2k)}_{m,1}$ *denote the image of the* $(m,1)$*-cable of the meridian in the* -1*-surgery on* J_{2k}*. Then we have*

$$\varphi_{i,j}(S^3_{-1}(J_{2k}), \mu^{(2k)}_{m,1}) = \begin{cases} 1 & \text{if } (i,j) = (k, m+k-1), \\ 0 & \text{if } i > k \text{ or } j > m+k-1. \end{cases}$$

Proof Since $\mathrm{CFK}^\infty(S^3, J_{2k}) \cong \mathrm{CFK}^\infty(S^3, T_{4k+1}) \oplus A$, by the filtered mapping cone formula, we have $\mathrm{CFK}^\infty(S^3_{-1}(J_{2k}), \mu^{(2k)}_{m,1}) \cong \mathrm{CFK}^\infty(S^3_{-1}(T_{4k+1}), \mu'^{(2k)}_{m,1}) \oplus A'$. By Lemma 2.1

$$\varphi_{i,j}(S^3_{-1}(J_{2k}), \mu^{(2k)}_{m,1}) = \varphi_{i,j}(X^\infty_n(T_{2,4k+1})\langle m-1\rangle).$$

According to Proposition 2.5, the value of $\varphi_{i,j}$ is determined by the sequence $\Delta_{k,m}(s)$ for $1 \le s \le m-1$. Note that $\Delta_{k,m}(1) = (k, m+k-1)$, and as s increases by 1 either the first or the second entry of $\Delta_{k,m}(s)$ decreases by 1. □

Proof of Theorem 1.2 Lemma 2.6 shows the $\varphi_{k,m+k-1}$ are linear independent, and the homomorphism

$$\bigoplus_{k>0,m>1} \varphi_{k,m+k-1} : \hat{\mathcal{C}}_{\mathbb{Z}}/\mathcal{C}_{\mathbb{Z}} \to \bigoplus_{k>0,m>1} \mathbb{Z}$$

is surjective. In particular, for each fixed $k > 0$ the homomorphism

$$\bigoplus_{m>1} \varphi_{k,m+k-1} : \hat{\mathcal{C}}_{\mathbb{Z}}/\mathcal{C}_{\mathbb{Z}} \to \bigoplus_{m>1} \mathbb{Z}$$

is surjective. □

3 Blowing down two-bridge links

We now turn to the algorithm due to Ozsváth, Szabó and Hales. Let $R = R_1 \cup R_2$ be a two-bridge link, where R_1 and R_2 are the two link components. One can view R as two arcs A_1 and A_2 on a fixed S^2 with two trivial over-arcs C_1 and C_2 each intersecting S^2 transversely at end points, such that $R_i = A_i \cup C_i$.

Since R_2 is unknotted, ϵ-framed surgery on R_2 with $\epsilon = \pm 1$ recovers S^3. Let Σ be the genus-one surface obtained from S^2 by attaching a one-handle along the arc C_2, and let μ_2 be the meridian of the one-handle. Ozsváth and Szabó give a description for a genus-one doubly pointed Heegaard diagram for the knot R_1 in $S^3_\epsilon(R_2) = S^3$ as follows.

Proposition 3.1 [16, Proposition 6.3] *For $\epsilon = \pm 1$, let $\alpha = C_2 \cup (\text{trivial arc in } S^2)$, $\beta = A_2 \cup C_2 \cup k\mu_2$, where k is chosen such that $\alpha \cdot \beta = \epsilon$, and put z and w basepoints at the two end points of C_1. Then $(\Sigma, \alpha, \beta, z, w)$ represents $(S^3_\epsilon(R_2), R_1)$.*

Proof Clearly (Σ, α, β) represents $S^3_\epsilon(R_2)$. Connecting z to w in the complement of α traces out C_1 while connecting w to z in the complement of β traces out A_1. □

In particular, it follows that $(S^3_\epsilon(R_2), R_1)$ is a $(1,1)$ knot. Next, view the two-bridge link R as the numerator closure of a rational tangle p/q, with p even and q odd. We follow the convention in [12]. Every rational tangle can be obtained from the trivial tangle by performing

- the vertical right-handed half-twist τ and its reverse τ^{-1};
- the horizontal left-handed half-twist σ and its reverse σ^{-1}.

Specifically in the case when the numerator closure is a link, τ^2 and σ (and their reverses) suffice to generate the rational tangle.[1] This can be seen from a simple lemma regarding continued fractions, as follows. For integers $a_1, \dots, a_\ell$, denote by $[a_1, \dots, a_\ell]$ the continued fraction

$$a_1 + \cfrac{1}{a_2 + \cfrac{1}{\cdots + \cfrac{1}{a_{\ell-1} + \cfrac{1}{a_\ell}}}}.$$

Lemma 3.2 *If p is even and q is odd, we can arrange such that $p/q = [a_1, \dots, a_\ell]$ where ℓ is odd, and a_i is even when i is odd.*

Proof Set $(p_0, q_0) = (p, q)$, and for each $i \geq 1$, we will recursively choose integers (a_i, p_i, q_i) with p_i and q_i coprime, such that

$$\frac{p_{i-1}}{q_{i-1}} = a_i + \frac{q_i}{p_i}. \tag{20}$$

Since p_{i-1}/q_{i-1} is between two consecutive integers, we choose a_i simply to be the closest even integer (resp. the closest integer) when i is odd (resp. when i is even) and choose p_i, q_i according to (20). It follows that $|p_i| = |q_{i-1}|$ and

$$p_{i-1} = a_i q_{i-1} + q_i \mod 2.$$

[1] In fact τ^2 and σ^2 and their reverses suffice, but at the expense of increasing the length of the continued fraction. For our purpose we will use τ^2 and σ.

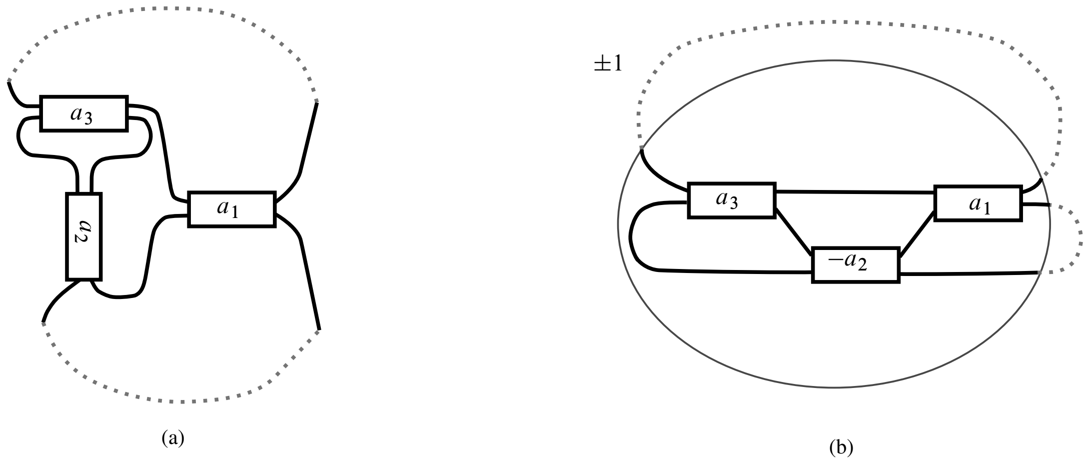

Figure 3: On the left, a rational tangle in the standard representation [12] corresponding to $p/q = [a_1, a_2, a_3]$, where positive numbers indicate crossings of the type ╳ and negative numbers vice versa. The diagram is alternating if all a_i are of the same sign. On the right, the same tangle in the 3-strand-braid representation [12]. The numbers in the boxes indicate the number of right-handed half-twists. The numerator closure of the tangle, indicated by the dotted lines, is a two-bridge link. For even a_1 and a_3, the knot $K^{\pm}[a_1, a_2, a_3]$ is obtained by doing ± 1 surgery on one of the components.

From these one can inductively show that for all $0 \le i \le n$ we have

$$(p_i, q_i) = \begin{cases} (\text{even}, \text{odd}) & \text{if } i \text{ is even}, \\ (\text{odd}, \text{even}) & \text{if } i \text{ is odd}. \end{cases}$$

Note that $|q_i| < |p_i| = |q_{i-1}|$, and therefore this process will terminate in finite number of steps. Also the last term a_n must have n odd, since $q_n = 0$ which is an even number. □

Definition 3.3 Denote by $K^{\pm}([a_1, \dots, a_\ell])$ the knot obtained by doing ± 1 surgery on the upper strand of the numerator closure of tangle $p/q = [a_1, \dots, a_\ell]$, respectively. One can also write $K^{\pm}(p/q)$. See Figure 3(b).

3.1 A diagrammatic algorithm

The following algorithm is due to Jonathan Hales [8]. Let us consider the effect of action τ^2 and σ on the Heegaard diagram $(\Sigma, \alpha, \beta, z, w)$ inside $\epsilon = \pm 1$ surgery. We depict the result of these actions in Figure 4. Note that in Figure 4(b) and (c), in order to preserve the framing of β curve, for each added full twist we need to "double-back" one time such that the intersection points cancel in pairs with sign, and the framing of the β curve remains to be ϵ.

In order to compute the Heegaard Floer homology of a $(1, 1)$ knot, the standard treatment is to lift the genus-one Heegaard diagram $(\Sigma, \alpha, \beta, z, w)$ to the universal cover $\mathbb{R}^2$, where the bigon counts are explicit. Therefore we would like to study the actions of τ^{2n} and σ on the universal cover of Σ. The following is interpreted from [8, Lemma 3.2.3]:

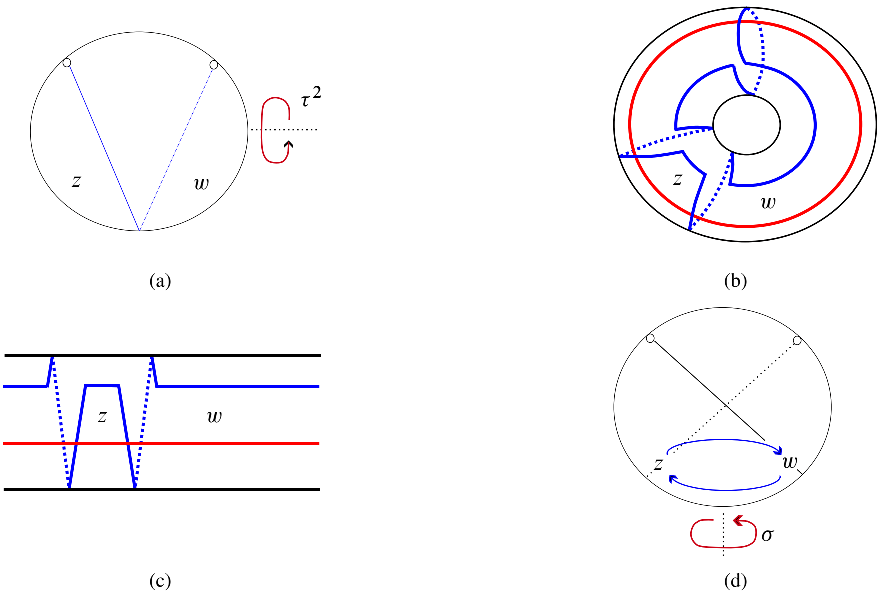

Figure 4: (a) and (b) demonstrate the result of applying τ^2 on the four-punctured sphere and $\Sigma = S^3 \cup$ (one-handle) supposing $\epsilon = +1$, respectively. In (d) the two black arcs illustrate the effect of σ.

First note that all of the following transformations keep the lifts of α unchanged, and deform only the lifts of β.

For $n \in \mathbb{Z}$, τ^{2n} has the following effect: In the covering $S^1 \times \mathbb{R} = [0,1] \times \mathbb{R}/\{(0,r) \sim (1,r) \mid r \in \mathbb{R}\}$, where the lifts of α are identified with $S^1 \times \mathbb{Z}$, arrange such that the lifts of the z basepoint lie on a vertical line $\ell_z := \{1/4\} \times \mathbb{R}$ and the lifts of the w basepoint lie on a vertical line $\ell_w := \{3/4\} \times \mathbb{R}$. Fixing $\widetilde{\alpha}$, z and w basepoints, perform an ambient isotopy in a small neighborhood of ℓ_z given by the following: fix a small $\varepsilon > 0$,

$$H_t^{(z)}(x,r) = \begin{cases} \left(x, r + \left(1 - \frac{\left|\frac{1}{4} - x\right|}{\varepsilon}\right) nt\right) & \text{if } x \in \left[\frac{1}{4} - \varepsilon, \frac{1}{4} + \varepsilon\right], \\ (x,r) & \text{otherwise,} \end{cases} \tag{21}$$

for $0 \le t \le 1$. In the process, a small neighborhood of $\tilde{\beta}$ near each intersection point $\tilde{\beta} \cap \ell_z$ is shifted vertically by $|n|$ units and crosses $|n|$ of the z basepoints. Equivalently, τ^{2n} can also be interpreted as follows. Fixing $\widetilde{\alpha}$, z and w basepoints, perform an ambient isotopy in a small neighborhood of ℓ_w given by the following: fix a small $\varepsilon > 0$,

$$H_t^{(w)}(x,r) = \begin{cases} \left(x, r - \left(1 - \frac{\left|\frac{3}{4} - x\right|}{\varepsilon}\right) nt\right) & \text{if } x \in \left[\frac{3}{4} - \varepsilon, \frac{3}{4} + \varepsilon\right], \\ (x,r) & \text{otherwise,} \end{cases} \tag{22}$$

for $0 \le t \le 1$. In the process, a small neighborhood of $\tilde{\beta}$ near each intersection point $\tilde{\beta} \cap \ell_w$ is shifted vertically by $|n|$ units and crosses $|n|$ of the w basepoints. Further lift this to the universal cover $\mathbb{R}^2$. For an example, see Figure 6 in Example 4.2 and Figure 11.

On the other hand, note that σ is a local action. See Figure 4(d). In the universal cover, σ (resp. σ^{-1}) corresponds to performing a clockwise (resp. counterclockwise) half-Dehn twist around each lift of z and w basepoints. See the middle step of Figure 11. As a convention in this paper, after each action of σ we also switch the role of z and w basepoints, such that z is on the left and w is on the right. The switching induces a chain homotopy equivalence of the resulting Heegaard Floer complex. We include the switching such that the z basepoint is consistently on the left and w basepoint is consistently on the right in each lift.

According to Lemma 3.2, each rational tangle whose numerator closure is a two-component link can be obtained from the trivial tangle by applying τ^2 and σ iteratively. Therefore we have described an algorithm that produces the $(1,1)$ diagram of any knot that arises from blowing down a two-bridge link. Here by a $(1,1)$ diagram, we mean the universal cover of a genus-one doubly pointed Heegaard diagram, where we fix a preferred parametrization. We have outlined a proof for the following theorem:

Theorem 3.4 [8] *The actions τ^2 and σ provide an explicit description of the $(1,1)$ diagram of any knot that arises from blowing down a two-bridge link.*

4 Classifying $K^{\pm}(p/q)$ with continued fraction length ≤ 3

Using the algorithm due to Ozsváth, Szabó and Hales, the goal of this section is to give a complete classification of $\mathrm{CFK}^{\infty}(S^3, K^{\pm}(p/q))$ for $p/q = [a_1, \dots, a_\ell]$ where $\ell = 1$ or 3 and a_i is even for each odd i. Note that

$$K^-(p/q) = -K^+(-p/q) = -K^+([-a_1, \dots, -a_\ell]). \tag{23}$$

As a road map for this section, we will first consider the case $\ell = 1$ in the next subsection. Then, in Section 4.2, we will discuss some general facts about the $\ell = 3$ case, reducing it to five subcases. Finally we will prove each one of these subcases in Sections 4.3 through 4.7, completing the classification. All five subcases and their corresponding conclusions are recorded in Proposition 4.13 for the reader's convenience.

4.1 Case $K^{\pm}([a_1])$

The following proposition together with (23) classify all the $K^{\pm}([a_1])$.

Proposition 4.1 *For $n > 0$,*

$$K^+([2n]) = -T_{n-1,n}, \tag{24}$$

$$K^+([-2n]) = -T_{n,n+1} \tag{25}$$

and $K^+([0])$ is the unknot.

Proof We will only prove (24). The other case is similar and left for the reader. Recall that the torus knot $-T_{n,n-1}$ is the braid closure of $(\omega_{n-1} \cdots \omega_1)^{n-1}$ where ω_i is the braid group element that exchanges the i-th and $(i+1)$-th strand, with the crossing convention given by Figure 5(b). Note that a left-handed full twist of the first k strands has a presentation of $(\omega_{k-1} \cdots \omega_1)^k$.

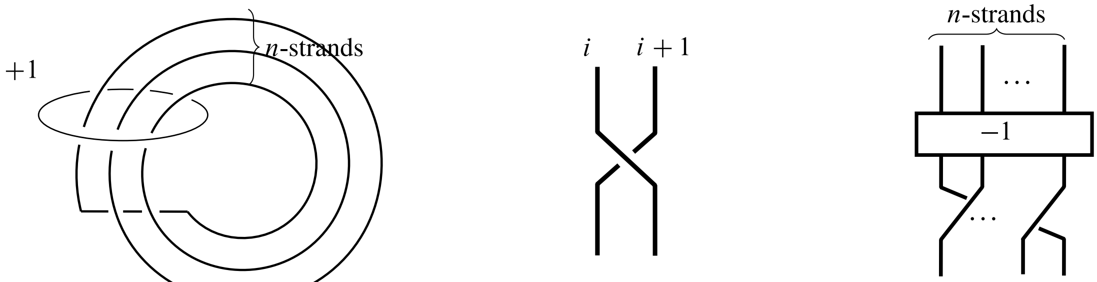

(a) the knot $K^+([2n])$ (b) the braid group element ω_i (c) a braid presentation of $K^+([2n])$

Figure 5: Illustrations for the proof of Proposition 4.1.

As depicted in Figure 5(c), the knot $K^+([2n])$ is the braid closure of $\omega_1\omega_2\cdots\omega_{n-1}(\omega_{n-2}\cdots\omega_1)^{n-1}$. Therefore it suffices to show that as elements of the braid group

$$(\omega_{n-1}\cdots\omega_1)^{n-1} = \omega_1\omega_2\cdots\omega_{n-1}(\omega_{n-2}\cdots\omega_1)^{n-1}. \tag{26}$$

From the braid relation

$$\omega_i\omega_{i+1}\omega_i = \omega_{i+1}\omega_i\omega_{i+1}, \tag{27}$$

it is straightforward to see that for $1 \le k < i \le k+j$,

$$\omega_i(\omega_k\omega_{k+1}\cdots\omega_{k+j}) = (\omega_k\omega_{k+1}\cdots\omega_{k+j})\omega_{i-1}. \tag{28}$$

We proceed by induction. For each $1 \le i \le n-1$, we claim that

$$(\omega_{n-1}\cdots\omega_1)^{n-1} = (\omega_{n-1}\cdots\omega_1)^{n-1-i}(\omega_{n-i}\cdots\omega_{n-1})(\omega_{n-2}\cdots\omega_1)^i. \tag{29}$$

This is obviously true for $i=1$. Suppose this is true for some $1 \le i \le n-2$. By using (28), we have

$$\begin{aligned}
&(\omega_{n-1}\cdots\omega_1)^{n-1}\\
&\quad= (\omega_{n-1}\cdots\omega_1)^{n-1-i}(\omega_{n-i}\cdots\omega_{n-1})(\omega_{n-2}\cdots\omega_1)^i\\
&\quad= (\omega_{n-1}\cdots\omega_1)^{n-2-i}\omega_{n-1}\cdots\omega_{n-i}(\omega_{n-i-1}\omega_{n-i}\cdots\omega_{n-1})\omega_{n-i-2}\cdots\omega_1(\omega_{n-2}\cdots\omega_1)^i\\
&\quad= (\omega_{n-1}\cdots\omega_1)^{n-2-i}(\omega_{n-i-1}\omega_{n-i}\cdots\omega_{n-1})(\omega_{n-2}\cdots\omega_{n-i-1})\omega_{n-i-2}\cdots\omega_1(\omega_{n-2}\cdots\omega_1)^i\\
&\quad= (\omega_{n-1}\cdots\omega_1)^{n-1-(i+1)}(\omega_{n-i-1}\cdots\omega_{n-1})(\omega_{n-2}\cdots\omega_1)^{i+1}.
\end{aligned}$$

Thus we have proved (29). Taking $i=n-1$ in (29) yields (26). □

Example 4.2 Consider $K^+([-2n])$ for $n>0$. Applying the algorithm by Ozsváth, Szabó and Hales, starting from a $(1,1)$ diagram for the unknot $K^+([0])$, where the β curve has slope -1, we equivariantly perform downwards finger moves of n units such that a small neighborhood of $\tilde{\beta}$ near each intersection point $\tilde{\beta}\cap\ell_z$ crosses n of the z basepoints. The resulting $(1,1)$ diagram is depicted in Figure 6. For a chosen lift $\tilde{\alpha}$ of α, we mark the intersection points of $\tilde{\alpha}\cap\tilde{\beta}$ from left to right by $x_1, x_2, \ldots$ in order.

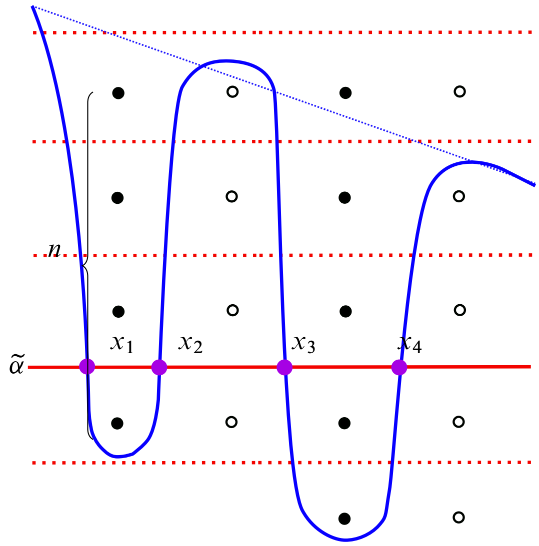

Figure 6: The $(1,1)$ diagram for $K^+([-2n])$ with $n > 0$, where the solid dots indicate (lifts of) the z basepoint and the hollow dots indicate (lifts of) the w basepoint.

There are $2n-1$ intersection points in total, and for each $i \in \{1, \dots, n-1\}$, there is a bigon from x_{2i-1} to x_{2i} with i copies of z and a bigon from x_{2i+1} to x_{2i} with $n-i$ copies of w; there are no other bigons. Therefore we conclude that $\mathrm{CFK}^\infty(S^3, K^+([-2n]))$ is generated by $x_1, \dots, x_{2n-1}$ with the differentials

$$\partial x_{2i-1} = x_{2i-2} + x_{2i}$$

and the filtration shifts

$$\Delta_{\mathcal{I},\mathcal{J}}(x_{2i-1}, x_{2i-2}) = (n-i+1, 0),$$
$$\Delta_{\mathcal{I},\mathcal{J}}(x_{2i-1}, x_{2i}) = (0, i)$$

for $i = 0, \dots, n$, where we take $x_0 = x_{2n} = 0$. For the definition of $\Delta_{\mathcal{I},\mathcal{J}}$, see Definition 2.2.

From Proposition 4.1 we already know $K^+([-2n]) = -T_{n,n+1}$. So this provides another way of computing the knot Floer complex of $T_{n,n+1}$ torus knots independent of the structure theorem of L-space knots [17] and the computation of their Alexander polynomials.

In the other direction, without knowing $K^+([-2n]) = -T_{n,n+1}$, just by looking at their $(1,1)$ diagrams in Figure 6, one can also show they are L-space knots via [7, Theorem 1.2] (the $(1,1)$ diagram is coherent) and this gives a shortcut for computing their Alexander polynomials.

4.2 General results on the case $\ell = 3$

From now on we fix the length of the continued fraction to be 3. Note that $K^\pm([2n_1, 0, 2n_2]) = K^\pm([2n_1 + 2n_2])$, and therefore the results here also apply to the knots in the previous section. We will end up reducing the classification to the case when $a_2 = \pm 1$ or 0, so for the following lemma we consider some relations between this subclass of knots.

Lemma 4.3 *For any integer* b, n, n_1 *and* n_2, *we have*

$$K^{\pm}([2n_1, b, 2n_2]) = K^{\pm}([2n_2, b, 2n_1]), \tag{30}$$

$$K^{\pm}([2n_1, 1, 2n_2]) = K^{\pm}([2(n_1+1), -1, 2(n_2+1)]), \tag{31}$$

$$K^{\pm}([0, \pm 1, 2n]) = K^{\pm}([2n]), \tag{32}$$

$$K^{\pm}([2, -1, 2n]) = K^{\pm}([2n-2]), \tag{33}$$

$$K^{\pm}([-2, 1, 2n]) = K^{\pm}([2n+2]), \tag{34}$$

$$K^{+}([2n_1, 1, 2n_2]) = -K^{-}([-2n_1, -1, -2n_2]). \tag{35}$$

Proof The relation (30) can be seen by rotating the paper plane by 180 degrees along a vertical axis. To show (31), we compute

$$\begin{aligned}[2(n_1+1), -1, 2(n_2+1)] &= 2(n_1+1) + \cfrac{1}{-1 + \cfrac{1}{2(n_2+1)}} \\ &= \frac{-4(n_1+1)(n_2+1) + 2(n_1+1) + 2(n_2+1)}{1 - 2(n_2+1)} = \frac{4n_1n_2 + 2n_1 + 2n_2}{2n_2+1} \\ &= [2n_1, 1, 2n_2].\end{aligned}$$

The relation (32) is clear from the link diagram. Relations (33) and (34) are straightforward from the continued fraction. Relation (35) comes from mirroring. □

4.2.1 Full Dehn twists Let $\mathcal{H}^{\pm}([2n_1, b, 2n_2])$ denote the lifted Heegaard diagram in $S^1 \times \mathbb{R}$ obtained by applying the action $\tau^{2n_2}\sigma^b\tau^{2n_1}$ over the ∓ 1 sloped curve $\tilde{\beta}$. By default, we also fix a preferred lift $\tilde{\alpha}$ of α and $\tilde{\beta}$ of β. According to the algorithm discussed in Section 3.1, with the above data, $\mathcal{H}^{\pm}([2n_1, b, 2n_2])$ induces a basis B for the knot Floer complex $\mathrm{CFK}^{\infty}(S^3, K^{\pm}([2n_1, b, 2n_2]))$

When $b = \pm 1$ or 0, after performing τ^{2n_1}, connect each pair of the z and w basepoint with a horizontal line segment γ. After potentially pulling tight $\tilde{\beta}$, we see that γ intersects $\tilde{\beta}$ at most once. See Figure 7(a) for the case when $b = 1$; the other two cases are similar. The action of σ^2 is given by the local transformation depicted in Figure 7(b). Since this transformation is defined inside a small neighborhood of γ, we may reverse the order the operations, i.e., $\tau^{2n_2}\sigma_{\gamma}^2\tau^{2n_1} = \sigma_{\gamma'}^2\tau^{2n_2}\tau^{2n_1}$. Here we write σ_{γ} to stress the region where we perform the local transformation, and γ' is the image of γ under the ambient isotopy τ^{2n_2} given by (21) or (22). In other words, after performing τ^{2n_1}, instead of performing σ_{γ}^2 first, we can apply the ambient isotopy τ^{2n_2} to $\tilde{\beta}$ and γ at the same time, then apply $\sigma_{\gamma'}^2$ in a small neighborhood of γ'. This has the same effect as performing σ_{γ}^2 first, followed by τ^{2n_2}. Once the regions of the operations are understood, we drop them from the indices of σ.

Definition 4.4 For an arc γ, define ρ_+ to be the conformal transformation in a neighborhood of γ depicted in Figure 7(b). This is to be understood up to rotation in $\mathbb{R}^2$. We can similarly define ρ_-, given by a reflection of ρ_+ along a vertical axis. The action $\rho_{\pm}$ is trivial if $\tilde{\beta} \cap \gamma_{\pm} = \varnothing$.

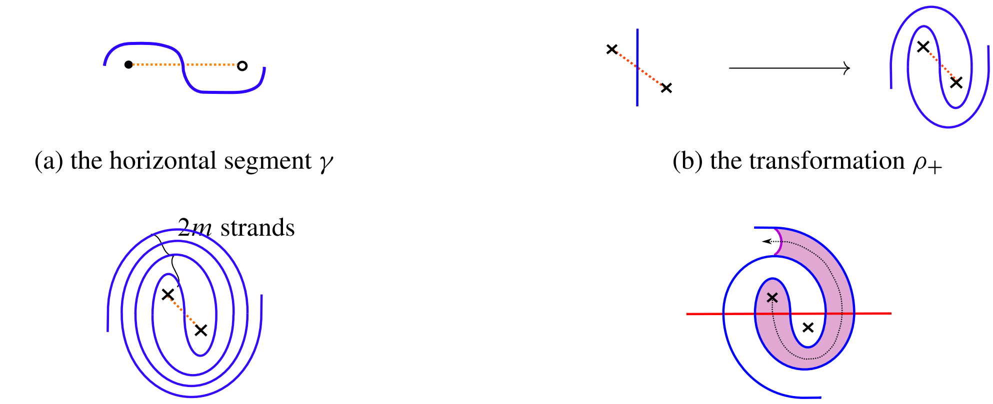

(a) the horizontal segment γ

(b) the transformation ρ_+

(c) the result after performing ρ_+^m

(d) a counterclockwise finger move

Figure 7: In the above diagrams, the $\times$ symbol is used to indicate either basepoint.

Remark 4.5 A useful perspective is to view ρ_+ as the reverse of the counterclockwise finger move depicted in Figure 7(d), where we move both the basepoint and the $\tilde{\beta}$ curve. Equivalently one can also perform a counterclockwise finger move on the other basepoint to achieve the same result. Similar statements are true for ρ_-, with the only difference being that the finger move is clockwise.

We stress that $\rho_\pm$ preserves the angle between $\tilde{\beta}$ and γ. For example $\rho_- \circ \rho_+$ is not well defined. Nevertheless, this allows us to reduce any $\mathcal{H}^\pm([2n_1, b, 2n_2])$ to the case when $b = \pm 1$ or 0.

For the following, set $\epsilon = \operatorname{sgn}(b)$, $m = \lfloor \epsilon b/2 \rfloor$ and $b' = b - 2\epsilon m$. To understand $\mathcal{H}^\pm([2n_1, b, 2n_2])$, it suffices to understand $\mathcal{H}^\pm([2n_1, b', 2n_2])$ and the action ρ_ϵ^m over certain arcs (the image of all the γ under τ^{2n_2}).

Definition 4.6 When $b' = 1$ or 0, define γ_ϵ to be a straight line segment of slope $-2n_2$ from a z basepoint to a w basepoint in $\mathcal{H}^\pm([2n_1, 1, 2n_2])$.

When $b' = -1$, define γ_- to be a straight line segment of slope $-2(n_2 - 1)$ from a z basepoint to a w basepoint in $\mathcal{H}^\pm([2(n_1 - 1), 1, 2(n_2 - 1)])$.

We abuse the notation and let $\gamma_\pm$ also denote the line segments with the same slope in $\mathcal{H}^\pm([2n_1, b, 2n_2])$.

Lemma 4.7 *Given n_1, b and n_2, for m and b' as above,*

- *when $b \geq 0$, $\mathcal{H}^\pm([2n_1, b, 2n_2])$ is obtained from $\mathcal{H}(K^\pm([2n_1, b', 2n_2]))$ by performing the local transformation ρ_+^m over all γ_+;*
- *when $b \leq 0$, $\mathcal{H}^\pm([2n_1, b, 2n_2])$ is obtained from $\mathcal{H}(K^\pm([2n_1, b', 2n_2]))$ by performing the local transformation ρ_-^m over all γ_-.*

Proof The case when $b' = 0$ or 1 follows from the fact that $\tau^{2n_2}\sigma^b\tau^{2n_1} = \sigma^{2m}\tau^{2n_2}\sigma^{b'}\tau^{2n_1}$ and the image of γ under τ^{2n_2} is γ_+. Consider the case when $b' = -1$. We already know that

$$K^\pm([2n_1, -1, 2n_2]) = K^\pm([2(n_1 - 1), 1, 2(n_2 - 1)]).$$

In fact, one can check that after pulling tight $\tilde{\beta}$, $\mathcal{H}^{\pm}([2n_1,-1,2n_2])$ and $\mathcal{H}^{\pm}([2(n_1-1),1,2(n_2-1)])$ represent the same diagram. This justifies the definition of γ_- in this case and the rest of the proof follows. □

The maps defined in Lemma 4.7 are equivariant; denote them by $\sigma^{\pm 2m}$, respectively. It turns out that they induce maps on the knot Floer chain complex together with certain *marked basis*, which we will now define.

We describe the process of assigning $+$ markings; the $-$ case is parallel.

Definition 4.8 For a given γ_+, after pulling tight $\tilde{\beta}$, let $a_+ = \gamma_+ \cap \tilde{\alpha}$ and $b_+ = \gamma_+ \cap \tilde{\beta}$. Both a_+ and b_+ are unique if they exist, as can be seen from the local picture Figure 7(a). From Figure 7(d) we can see that ρ_+ does not affect the knot Floer complex if $\tilde{\alpha} \cap \gamma_+ = \varnothing$. We give a $+$ marking to the "closest" intersection point p of $\tilde{\alpha} \cap \tilde{\beta}$ to a_+ or b_+. Concretely, p is the unique intersection point that forms a (α,β,γ) triangle with a_+ and b_+. We call p a $+$ marked point.

For the chain complex $C = \mathrm{CFK}^{\infty}(S^3, K^{\pm}([2n_1,b,2n_2]))$ with the basis B induced by $\tilde{\alpha}$ and $\tilde{\beta}$, assign markings for every γ_+. This results in a $+$ marked basis B_+. Note that it is possible for a basis element to be assigned more than one $+$ marking.

Similarly define intersection points a_-, b_- as the $-$ marked points and B_- as a $-$ marked basis.

Let D_1 be the filtered chain complex over $\mathbb{F}[U,U^{-1}]$ generated by x_0, x_1, x_2 and y with differentials (each with length one) as below

$$\begin{tikzcd} x_0 \arrow[d] & x_1 \arrow[l] \arrow[d] \\ y & x_2 \arrow[l] \end{tikzcd}$$

Namely, D_1 is a length-one box summand.

Lemma 4.9 *Given a_1, a_3 even and $a_2 \geq 0$, we can obtain a model of $\left(\mathrm{CFK}^{\infty}(K^{\pm}([a_1,a_2+2,a_3])), B'_+\right)$ from $\left(\mathrm{CFK}^{\infty}(K^{\pm}([a_1,a_2,a_3])), B_+\right)$ as follows. For each $+$ marked point p, add ℓ copies of D_1 summands, where ℓ is the number of $+$ markings of p, such that for each D_1 summand, y and p share the same filtration level and Maslov grading. Remove all the previous markings and assign a $+$ marking to x_1 of each added D_1 summand. This gives the new marked basis B'_+.*

Proof Given a intersection point $b_+ = \gamma_+ \cap \tilde{\beta}$ for some γ_+, let p be the $+$ marked point induced by γ_+. In a small neighborhood of γ_+, the transformation ρ_+ is given by Figure 8(a), up to rotation in $\mathbb{R}^2$. In the resulting diagram, label the intersection points by p_0, c, a, b and p_1 from left to right (as we will see, this assignment also only matters up to the symmetry from the middle). They generate a complex depicted in Figure 8(b). In particular, we can perform a change of basis $\{a,b,c,p_0,p_1\} \mapsto \{a,b,c,p_0+p_1,p_i\}$ where $i=0$ or 1. Both choice of the change of basis splits off a summand generated by $\{a,b,c,p_0+p_1\}$ isomorphic to D_1. We then identify either p_0 or p_1 with p. For $i=0,1$, clearly p_0+p_1 share the same filtration level and Maslov grading with p_i; moreover observe that p_i inherits all the bigons of p (either incoming or outgoing, with the same filtration shifts). Adopting the perspective of Figure 7(d),

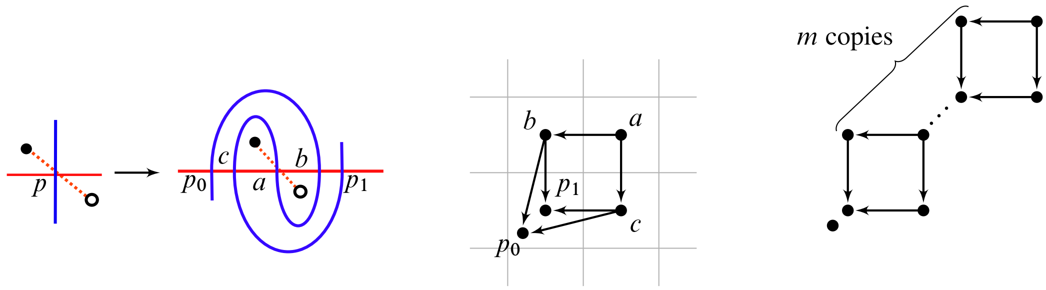

(a) (b) (c) the effect of the map σ^{2m}

Figure 8: The effect on CFK^∞.

performing a counterclockwise finger move will undo the transformation ρ_+ on the diagram level, and remove a box summand on the chain complex level. The choice of basepoint with which we perform the finger move corresponds to identifying p with p_0 or p_1.

Over the diagram $\mathcal{H}^\pm([a_1, a_2+2, a_3])$, following $\tilde\beta$ and record the sequence of b_+ in order. Perform the finger move in Figure 7(d) near each b_+ (this amounts to removing an interval of $\tilde\beta$ near b_+ and gluing it back). The resulting diagram is $\mathcal{H}^\pm([a_1, a_2, a_3])$. This proves the statement regarding the chain complex. For the new marked basis B'_+, simply notice that in the local picture Figure 8(a), the intersection point a forms a triangle with a_+ and b_+. □

Lemma 4.10 *Given a_1, a_3 even and $a_2 \le 0$, we can obtain a model of $\big(\mathrm{CFK}^\infty(K^\pm([a_1, a_2+2, a_3])), B'_-\big)$ from $\big(\mathrm{CFK}^\infty(K^\pm([a_1, a_2, a_3])), B_-\big)$ as follows. For each $+$ marked point p, add ℓ copies of D_1 summands, where ℓ is the number of $-$ markings of p, such that for each D_1 summand, x_1 and p share the same filtration level and Maslov grading. Remove all the previous markings and assign a $-$ marking to y of each added D_1 summand. This gives the new marked basis B'_-.*

Proof This is parallel to Lemma 4.9. □

Practically, we only need to consider the complex with marked basis $\big(\mathrm{CFK}^\infty(K^\pm([2n_1, b', 2n_2])), B_\pm\big)$ with $b' = \pm 1$ and 0 and consider the map $\sigma^{\pm 2m}$. In general it is not difficult to determine $B_\pm$ using Definitions 4.6 and 4.8. In particular, we have proved the following.

Proposition 4.11 *Up to chain homotopy equivalence,*

$$\mathrm{CFK}^\infty(S^3, K^\pm([2n_1, b, 2n_2])) \cong \mathrm{CFK}^\infty(S^3, K^\pm([2n_1, b', 2n_2])) \oplus \bigoplus_{i=1}^{N} D_1,$$

where $b' = b - 2\epsilon m$ for $\epsilon = \mathrm{sgn}(b)$, $m = \lfloor \epsilon b/2 \rfloor$, N is the number of markings in the marked basis B_ϵ and D_1 is the length-one box complex.

For any n_1 and n_2, by Definition 4.6, γ_+ and γ_- coincide for $\mathrm{CFK}^\infty(K^\pm(S^3, [2n_1, 0, 2n_2]))$, so $B_+ = B_-$. In this case it is easy to check that the map σ^2 in Lemma 4.9 and the map σ^{-2} in Lemma 4.10 induce the same map on the level of filtered chain homotopy type, even though they induce different basis in the image. In other words, we have the following.

Lemma 4.12 *Up to filtered chain homotopy equivalence, for $n_1, n_2, b \in \mathbb{Z}$,*

$$\mathrm{CFK}^\infty(K^\pm(S^3, [2n_1, 2b, 2n_2])) \cong \mathrm{CFK}^\infty(K^\pm(S^3, [2n_1, -2b, 2n_2])).$$

Note that the marked bases B_+ and B_- are generally different for $\mathrm{CFK}^\infty(K^\pm([2n_1, 1, 2n_2]))$ since γ_+ and γ_- have different slopes.

In view of Lemmas 4.3, 4.9, 4.10 and 4.12 we can reduce the $\ell = 3$ case to some subcases as follows. Suppose we are given $[a_1, a_2, a_3]$ with $a_1, a_3 \in 2\mathbb{Z}$ and $a_2 \in \mathbb{Z}$. If a_2 is even, then it suffice to consider $a_2 > 0$, and by mirroring we only need to consider K^+. If a_2 is odd, by mirroring we can guarantee that $a_1 > 0$. Next reducing a_2 to the case $a_2 = \pm 1$, we can further restrict to the case $a_2 = 1$ and consider both B_+ and B_- on $\mathrm{CFK}^\infty(S^3, K^\pm([a_1, 1, a_3]))$. Finally note that we can require $a_3 \neq -2$.

In summary, we have the following five cases, which are the topics of the next five subsections, respectively. We record the conclusion of each subsection here for the reader's convenience. This, together with the $\ell = 1$ case completes the proof of Theorem 1.5.

Proposition 4.13 *According to the discussion above, the case $\ell = 3$ is fully classified by the following cases: for $n_1, n_2 \in \mathbb{Z}$ and integer $b > 0$,*

(1) $K^+([2n_1, 2b, 2n_2])$, *Corollary 4.17*;

for $n_1, n_2 > 0$,

(2) $K^+([2n_1, 1, 2n_2])$, *Proposition 4.27*;

(3) $K^-([2n_1, 1, 2n_2])$, *Proposition 4.31*;

and for $n_1 > 0, n_2 > 1$,

(4) $K^+([2n_1, 1, -2n_2])$, *Proposition 4.32*;

(5) $K^-([2n_1, 1, -2n_2])$, *Proposition 4.33.*

4.3 Case $K^+([2n_1, 2b, 2n_2])$ with $b > 0$

Since $K^+([2n_1, 0, 2n_2]) = K^+([2n])$ for $n = n_1 + n_2$, with $K^+([2n])$ already classified in Section 4.1, the only extra data we require is a set of markings on $\mathrm{CFK}^\infty(S^3, K^+([2n]))$ (which as complexes of L-space knots, admits a unique basis).

4.3.1 Marked basis for $K^+([-2n])$ with $n > 0$ Fix $-n = n_1 + n_2$ and let $n_2 = -k$ for $k \in \mathbb{Z}$. We seek to decide the marked basis corresponding to $K^+([-2(n-k), 2b, -2k])$ for $b > 0$. By Definition 4.6 γ_+ is of slope k. Revisit Figure 6: in a $S^1 \times \mathbb{R}$ slice, denote the lifts of α that intersect a chosen lift $\tilde{\beta}$ of β by α_1 through α_n from bottom to top. Fix a lift $\tilde{\alpha}$ of α. It takes n iterations to cover all the intersections of $\tilde{\alpha} \cap \tilde{\beta}$, with $\tilde{\alpha}$ being identified with α_ℓ for $1 \leq \ell \leq n$ in each iteration. In total there are $2n-1$ generators in the complex $\mathrm{CFK}^\infty(S^3, K^+([-2n])) = \mathrm{CFK}^\infty(S^3, T_{n,n+1})$. Every iteration covers 2 intersection points except the last one, which covers 1 intersection point.

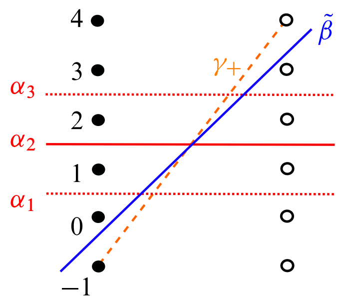

Figure 9: The γ_+ line segment with slope $n+1$ intersects the n sloped $\tilde\beta$ line segment once.

The only intersection points that are marked are the ones in the middle of each $S^1 \times \mathbb{R}$ slice. We focus on the portion of $\tilde\beta$ that travels between z and w basepoints, which is isotopic to a slope n line segment. The question of how many markings each intersection point receives is a completely combinatorial one: for each α_ℓ we need only count the number of line segments of slope k that intersect both line segments of slope n and slope 0.

In the below proposition, note that $\mathrm{CFK}^\infty(S^3, T_{n,n+1})$ admits a unique basis, and by the symmetry it does not matter from which end we start counting the generators.

Proposition 4.14 *For $n, b > 0$ and $k \in \mathbb{Z} \setminus \{0, n\}$, corresponding to $K^+([-2(n-k), 2b, -2k])$, the (2ℓ)-th generator in $\mathrm{CFK}^\infty(S^3, T_{n,n+1})$ receives $m(n,k,\ell)$ markings for $1 \le \ell \le n-1$, where*

$$m(n,k,\ell) = \begin{cases} k-n & \text{if } k \ge n+1, \\ n-\ell+\min\{\ell-k,0\}+\min\{k+\ell-n,0\} & \text{if } 1 \le k \le n-1, \\ -k & \text{if } k \le -1. \end{cases} \tag{36}$$

Proof For $1 \le \ell \le n-1$, in the ℓ-th iteration, α_ℓ is identified with $\tilde\alpha$ and the intersection point depicted in Figure 9 is the (2ℓ)-th generator. Label the height of the z and w basepoints by j, such that α_ℓ is between $j = \ell$ and $j = \ell - 1$.

When $k \ge n+1$, γ_+ intersects the line segment of slope n if and only if it starts from $j \le -1$ and ends at $j \ge n$. There are $k-1-n+1 = k-n$ of such line segments in total.

When $k \le -1$, γ_+ intersects the line segment of slope 0 if and only if it starts from $j \ge \ell$ and ends at $j \le \ell - 1$. There are $\ell - 1 - (\ell + k) + 1 = -k$ of such line segments in total.

When $1 \le k \le n-1$, γ_+ intersects both the line segments if only if it starts between $0 \le j \le \ell - 1$ and ends between $\ell \le j \le n-1$. In other words, we need only find the length of the interval $[k, k+\ell-1] \cap [\ell, n-1]$, which is given by

$$\min\{k+\ell-1, n-1\} - \max\{\ell, k\} + 1 = n - \ell + \min\{\ell-k, 0\} + \min\{k+\ell-n, 0\}. \qquad \square$$

Note that the expression $m(n,k,\ell)$ is symmetric under the transformations

$$(n,k,\ell) \mapsto (n,k,n-\ell), \quad (n,k,\ell) \mapsto (n,n-k,\ell).$$

4.3.2 Marked basis for $K^+([2n])$ with $n > 0$ This is similar to the previous case. Fix $n = n_1 + n_2$ and let $n_2 = -k$ for $k \in \mathbb{Z}$. We seek to decide the marked basis corresponding to $K^+([2(n+k), 2b, -2k])$ for $b > 0$. Similarly label the lifts of α by α_1 through α_{n-1} from bottom to top. It takes $n-1$ iterations to cover all the intersections of $\tilde{\alpha} \cap \tilde{\beta}$, with $\tilde{\alpha}$ being identified with α_ℓ for $1 \le \ell \le n-1$ in each iteration. In total there are $2n-3$ generators in the complex $\mathrm{CFK}^\infty(S^3, K^+([2n])) = \mathrm{CFK}^\infty(S^3, T_{n,n-1})$. Every iteration covers 2 intersection points except the last one, which covers 1 intersection point.

The only intersection points are the ones in the middle of each $S^1 \times \mathbb{R}$ slice and the portion of $\tilde{\beta}$ that travels between z and w basepoints is of slope $-n$. By Definition 4.6 γ_+ is of slope k. The proof of the next proposition is similar to the previous case and left to the reader as an exercise.

Proposition 4.15 *For $n, b > 0$ and $k \in \mathbb{Z} \setminus \{0, -n\}$, corresponding to $K^+([2(n+k), 2b, -2k])$, the $(2\ell-1)$-th generator in $\mathrm{CFK}^\infty(S^3, T_{n,n-1})$ receives $m'(n,k,\ell)$ markings for $1 \le \ell \le n-1$, where*

$$m'(n,k,\ell) = \begin{cases} -k-n & \text{if } k \le -n-1, \\ n-\ell+\max\{\ell-n-k, 0\}+\max\{k+\ell, 0\} & \text{if } -n+1 \le k \le -1, \\ k & \text{if } k \ge 1. \end{cases} \tag{37}$$

4.3.3 Marked basis for $K^+([0])$ Again let $n_2 = -k$ for $k \in \mathbb{Z}$.

Definition 4.16 Let C_0 be the complex generated by one element.

We seek to decide the marked basis in C_0 corresponding to $K^+([2k, 2b, -2k])$ for $b > 0$. Similar analysis as from the previous sections shows that the unique generator in C_0 is assigned $|k|$ markings for $k \in \mathbb{Z}$. This concludes the discussion of the case $K^+([2n_1, 2b, 2n_2])$ with $b > 0$. In particular, Propositions 4.14–4.15 and the above imply the following.

Corollary 4.17 *For any $n_1, n_2 \in \mathbb{Z}_{\neq 0}$ and $b > 0$, up to chain homotopy equivalence, the complex $\mathrm{CFK}^\infty\big(S^3, K^+([2n_1, 2b, 2n_2])\big)$ is given by,*

- *if $n_1 + n_2 = 0$,*
$$C_0 \oplus b|n_2|D_1;$$
- *if $n_1 + n_2 > 0$, defining $n = n_1 + n_2$ and $k = -n_2$,*
$$\mathrm{CFK}^\infty(S^3, T_{n,n-1}) \oplus b\bigg(\sum_{\ell=1}^{n-1} m'(n,k,\ell)\bigg)D_1,$$
where $m'(n,k,\ell)$ is given by (37);
- *if $n_1 + n_2 < 0$, defining $n = -(n_1 + n_2)$ and $k = -n_2$,*
$$\mathrm{CFK}^\infty(S^3, T_{n,n+1}) \oplus b\bigg(\sum_{\ell=1}^{n-1} m(n,k,\ell)\bigg)D_1,$$
where $m(n,k,\ell)$ is given by (36).

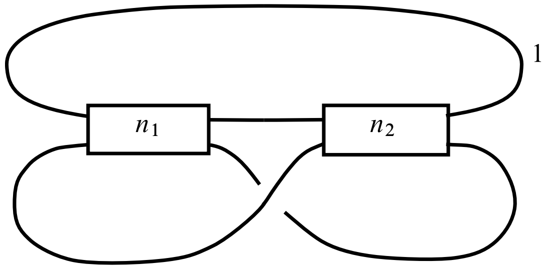

Figure 10: The knot $K^+_{n_1,n_2} = K^+([2n_1, 1, 2n_2])$. Numbers in the boxes indicate the number of right-handed full-twists.

4.4 Case $K^+([2n_1, 1, 2n_2])$ with $n_1, n_2 > 0$

From now on let us write $K^+_{n_1,n_2}$ for the knot $K^+([2n_1, 1, 2n_2])$ for the simplicity of the notation. See Figure 10 for a depiction of the knot $K^+_{n_1,n_2}$. Since the corresponding rational tangle has a presentation $[2n_1, 1, 2n_2]$, by Jonathan Hales's algorithm we shall consider the action $\tau^{2n_2}\sigma\tau^{2n_1}$ on the $(1, 1)$ diagram. The entire procedure is shown in Figure 11.

Fix a lift $\tilde{\alpha}$ (resp. $\tilde{\beta}$) of the α (resp. β) curve. Consider the final diagram in Figure 11 and suppose $\tilde{\beta}$ travels from left to right. Observe that in one iteration $\tilde{\beta}$ pass through $n_1 + n_2 - 1$ consecutive lifts of α (after isotoping away bigons without basepoint if necessary); denote them $\alpha_1, \dots, \alpha_{n_1+n_2-1}$ from bottom to top. To include all intersection points of $\tilde{\alpha} \cap \tilde{\beta}$, $n_1 + n_2 - 1$ iterations are needed. Following $\tilde{\beta}$, denote the diagram of each iteration by $H(s)$ for $1 \le s \le n_1 + n_2 - 1$; call it the s-th *block*. Note that in $H(s)$, $\tilde{\alpha}$ is identified with α_s.

To further determine the marked points, by Definition 4.6 each γ_+ is slope $-2n_2$, and viewing $\mathcal{H}^+([2n_1, 1, 2n_2])$ as $\mathcal{H}^+([2(n_1 + 1), -1, 2(n_2 + 1)])$, each γ_- is of slope $-2(n_2 + 1)$.

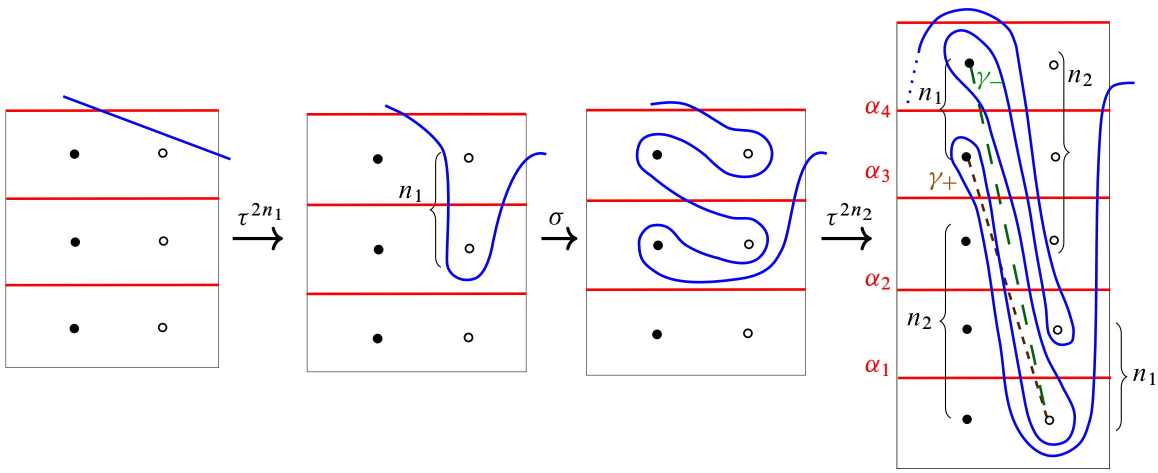

Figure 11: The action $\tau^{2n_2}\sigma\tau^{2n_1}$ when $n_1 = 2$ and $n_2 = 3$, starting from the slope -1. The solid dots indicate (lifts of) the z basepoint and the hollow dots indicate (lifts of) the w basepoint. The slope of γ_+ is $-n_2$ and the slope of γ_- is $-(n_2 + 1)$.

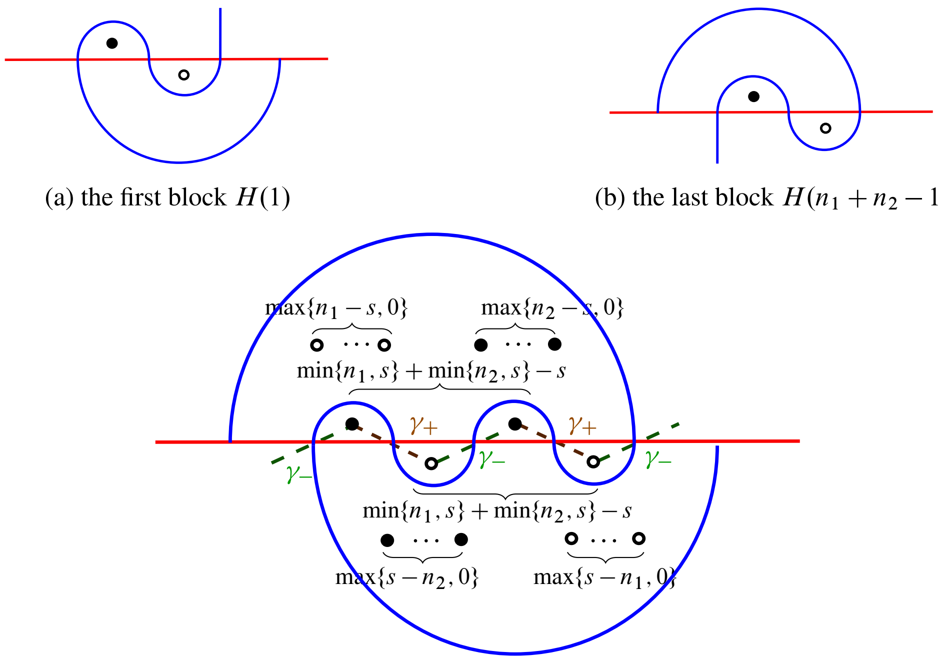

(a) the first block $H(1)$

(b) the last block $H(n_1 + n_2 - 1)$

(c) the s-th block $H(s)$ with $2 \le s \le n_1 + n_2 - 2$

Figure 12: Illustrations of blocks $H(s)$.

Lemma 4.18 *For $1 \le s \le n_1 + n_2 - 1$, each block $H(s)$ corresponds to the diagram depicted in Figure 12.*

Proof This can be readily read off from the final diagram in Figure 11. □

Remark 4.19 To obtain Figure 12, we are allowed to isotope the curves in the universal cover in the complement of the basepoints and other curves, and to move the basepoints around as long as they do not cross the curves. Since both these operations preserve the bigons, Figure 12 can be used to compute the knot Floer complex. We need to pay some extra attention to keep track of γ_+ and γ_-.

We now abuse the notation and denote the complex generated by $H(s)$ in $\mathrm{CFK}^\infty(S^3, K^+_{n_1,n_2})$ also by $H(s)$, for $1 \le s \le n_1 + n_2 - 1$. Define the chain complex $G(1) = \mathrm{CFK}^\infty(S^3, K^+_{n_1,n_2})$, and $G(i+1) = G(i)/(H(i) \cup H(n_1+n_2-i))$ for $1 \le i \le \lfloor \frac{n_1+n_2-1}{2} \rfloor$. Observe that $H(s)$ and $H(n_1+n_2-s)$ are both subcomplexes in $G(s)$.

We note that although suppressed from the notation, both $G(s)$ and $H(s)$ depend on s, n_1, n_2 and k.

Definition 4.20 Define a filtered chain complex D_s over $\mathbb{F}[U, U^{-1}]$ for $s \ge 1$ to be the complex generated by x_i with $0 \le i \le 2s$ and y, where differentials are given by

$$\begin{aligned} \partial x_{2i+1} &= x_{2i} + x_{2i+2}, && 0 \le i \le s-1, \\ \partial x_{2i} &= y, && 0 \le i \le s, \end{aligned}$$

with the filtration shifts

$$\begin{aligned}
\Delta_{\mathcal{I},\mathcal{J}}(x_{2i+1}, x_{2i}) &= (1,0), \\
\Delta_{\mathcal{I},\mathcal{J}}(x_{2i+1}, x_{2i+2}) &= (0,1), \qquad 0 \le i \le s-1, \\
\Delta_{\mathcal{I},\mathcal{J}}(x_{2i}, y) &= (i, s-i), \quad 0 \le i \le s.
\end{aligned}$$

We say D_s is supported in Maslov grading a and filtration level (i,j) if y is supported in Maslov grading a and filtration level (i,j).

Alternatively, D_s is the complex C_s with the addition of a generator y and the differentials from x_{2i} to y for $0 \le i \le s$ with above filtration shifts. The complex $D(3)$ is shown below as an example:

$$\begin{tikzcd}
x_0 \arrow[ddd] & x_1 \arrow[l] \arrow[d] & & \\
& x_2 \arrow[ddl] & x_3 \arrow[l] \arrow[d] & \\
& & x_4 \arrow[dll] & x_5 \arrow[l] \arrow[d] \\
y & & & x_6 \arrow[lll]
\end{tikzcd}$$

Lemma 4.21 *When $s \le \min\{n_1, n_2, \lfloor \frac{n_1+n_2-1}{2} \rfloor\}$, there exists a filtered change of basis T of $G(s)$, such that in the image of T, $H(s)$ becomes a summand, and moreover $H(s) \cong D_s$.*

Proof Consider two consecutive blocks $H(s)$ and $H(s+1)$ in $G(s)$ for $1 \le s \le \min\{n_1, n_2, \lfloor \frac{n_1+n_2-1}{2} \rfloor\}$. See Figure 13. Denote the intersection points of $\tilde{\beta} \cap \tilde{\alpha}$ by $x_0, \dots, x_{2s}, y, x'_0, \dots, x'_{2s'}, y'$ in order, where $s' = \min\{n_1, s+1\} + \min\{n_2, s+1\} - s - 1$, which is the number of small inner arcs in each half plane in $H(s+1)$. There are two cases to discuss: when $s = \min\{n_1, n_2\}$ or $s < \min\{n_1, n_2\}$.

- Suppose $s = \min\{n_1, n_2\}$. Then $s' = s$. Observe that the only arrows connected to $H(s)$ are given by

$$\partial x'_{2i} = y + y', \quad 0 \le i \le s.$$

Performing the change of basis

$$x'_i \mapsto x'_i + x_i, \quad 0 \le i \le 2s,$$

splits off $H(s)$ as a summand. Since the filtration shifts are

$$\Delta_{\mathcal{I},\mathcal{J}}(x_{2i}, y) = (i, s-i), \tag{38}$$

$$\Delta_{\mathcal{I},\mathcal{J}}(x'_{2i}, y) = (i, s-i) + (\max\{n_1 - s - 1, 0\}, \max\{n_2 - s - 1, 0\}) \tag{39}$$

for $0 \le i \le s$, this change of basis is filtered.

- Suppose $s < \min\{n_1, n_2\}$. Then $s' = s+1$. Similarly, the only arrows connected to $H(s)$ are given by

$$\partial x'_{2i} = y + y', \quad 0 \le i \le s+1.$$

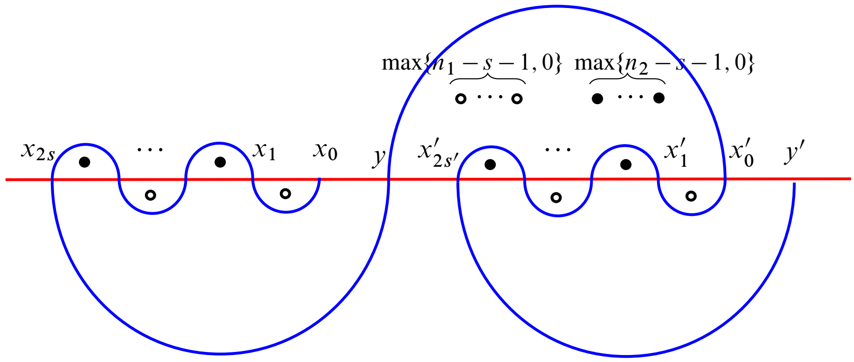

Figure 13: Two consecutive blocks $H(s)$ (on the left) and $H(s+1)$ (on the right) in $G(s)$ for $1 \le s \le \min\{n_1, n_2, \lfloor \frac{n_1+n_2-1}{2} \rfloor\}$. There could be other basepoints (at most more of each kind) in $H(s+1)$ in the lower half plane.

Performing the change of basis

$$x'_i \mapsto x'_i + x_i, \quad 0 \le i \le 2s,$$
$$x'_{2(s+1)} \mapsto x'_{2(s+1)} + x_{2s}$$

splits off $H(s)$ as a summand. Since the filtration shifts are

$$\Delta_{\mathcal{I},\mathcal{J}}(x_{2i}, y) = (i, s-i) \quad \text{for } 0 \le i \le s, \tag{40}$$
$$\Delta_{\mathcal{I},\mathcal{J}}(x'_{2i}, y) = (i, s+1-i) + (n_1 - s - 1, n_2 - s - 1) \quad \text{for } 0 \le i \le s+1, \tag{41}$$

this change of basis is filtered.

And it is clear from the diagram that each $H(s)$ generates a D_s summand (after quotienting out the top outmost arc). □

Lemma 4.22 *When $s \le \min\{n_1, n_2, \lfloor \frac{n_1+n_2-1}{2} \rfloor\}$, there exists a filtered change of basis T' of $G(s)$, such that in the image of T', $H(n_1+n_2-s)$ becomes a summand, and moreover $H(n_1+n_2-s) \cong D_s$.*

Proof This follows from Lemma 4.21 and the symmetry of the knot Floer complex. Equivalently one can run the similar argument as in the proof of Lemma 4.21 again. □

Lemma 4.23 *When $s \le \min\{n_1, n_2\} - 1$, there exists a filtered change of basis such that*

$$G(s) \cong G(s+1) \oplus H(s) \oplus H(n_1+n_2-s) \cong G(s+1) \oplus 2D_s.$$

Proof When $s \le \min\{n_1, n_2\} - 1$, we have $H(s) \cap H(n_1+n_2-1) = \varnothing$. By Lemmas 4.21 and 4.22, one simply applies the change of basis $T' \circ T$, and in the resulting complex $H(s)$ and $H(n_1+n_2-1)$ both become summands. □

These lemmas allow us to completely determine the complex $\mathrm{CFK}^\infty(S^3, K^+_{n_1,n_2})$. Due to (30), we may assume $n_1 \le n_2$. Therefore from now on we only consider knots of the form $K^+_{n,n+k}$ with $n > 0$ and $k \ge 0$.

Proposition 4.24 *For $n > 0$ and $k \geq 0$, we have*

$$\mathrm{CFK}^{\infty}(S^3, K^+_{n,n+k}) \cong G(n) \oplus 2\left(\bigoplus_{s=1}^{n-1} D_s\right).$$

Proof This follows from Lemma 4.23. Starting from $G(1) \cong \mathrm{CFK}^{\infty}(S^3, K^+_{n_1,n_2})$, we keep splitting off pairs of summands of D_s when $s \leq \min\{n_1, n_2\} - 1$. □

Therefore it suffices to determine the quotient complex $G(n) \cong \bigcup_{j=0}^{k} H(n+j)$ in $\mathrm{CFK}^{\infty}(S^3, K^+_{n,n+k})$. Note that the top outmost arc in $H(n)$ and the bottom outmost arc in $H(n+k)$ are quotiented out. We discuss several cases for different k.

- When $k = 0$, $G(n) \cong C_n$.
- When $k = 1$, we can use either Lemma 4.21 or 4.22 to split off a D_n summand. The remaining summand $G(n)/D_n$ is isomorphic to C_n.
- When $k = 2$, we can use Lemmas 4.21 and 4.22 to split off a pair of D_n summands. The remaining summand $G(n+1)$ is isomorphic to C_n.
- When $k > 3$, we again can use Lemmas 4.21 and 4.22 to split off a pair of D_n summands. The remaining summand is $G(n+1)$.

Definition 4.25 For $n > 0$, $k \geq 2$, define $C_{n,k}$ to be the complex generated by

$$\{x_i^{(j)} \mid 1 \leq j \leq k-1,\ 0 \leq i \leq 2n\} \cup \{y_j \mid 1 \leq i \leq k-2\}.$$

For simplicity, let $y_0 = y_{k-1} = 0$. For $1 \leq j \leq k-1$, the differentials are given by

$$\begin{aligned} \partial x_{2i+1}^{(j)} &= x_{2i}^{(j)} + x_{2i+2}^{(j)}, & 0 \leq i \leq n-1, \\ \partial x_{2i}^{(j)} &= y_j + y_{j-1}, & 0 \leq i \leq n, \end{aligned}$$

with the filtration shifts

$$\begin{aligned} \Delta_{\mathcal{I},\mathcal{J}}(x_{2i+1}^{(j)}, x_{2i}^{(j)}) &= (1,0), & \\ \Delta_{\mathcal{I},\mathcal{J}}(x_{2i+1}^{(j)}, x_{2i+2}^{(j)}) &= (0,1), & 0 \leq i \leq n-1, \\ \Delta_{\mathcal{I},\mathcal{J}}(x_{2i}^{(j)}, y_j) &= (i+j, n-i), & \\ \Delta_{\mathcal{I},\mathcal{J}}(x_{2i}^{(j)}, y_{j-1}) &= (i, k-j+n-i), & 0 \leq i \leq n. \end{aligned}$$

Note that $C_{n,2} = C_n$. See Figure 14(b) for an example when $n = 2$ and $k = 4$.

Lemma 4.26 *When $k \geq 2$, in $\mathrm{CFK}^{\infty}(S^3, K^+_{n,n+k})$ the quotient complex $G(n+1)$ is isomorphic to $C_{n,k}$.*

Proof The quotient complex $G(n+1) \cong \bigcup_{j=1}^{k-1} H(n+j)$ in $\mathrm{CFK}^{\infty}(S^3, K^+_{n,n+k})$. We have drawn the block $H(n+j)$ for $1 \leq j \leq k-1$ in Figure 14(a). Again the top outmost arc in $H(n+1)$ as well as the bottom outmost arc in $H(n+k-1)$ are quotiented out. Denoting the generators in $H(n+j)$ by $x_{2n}^{(j)}, \ldots, x_0^{(j)}, y_j$ from left to right in order, note that for each j the $2n+1$ generators $x_{2n}^{(j)}, \ldots, x_0^{(j)}$ form a

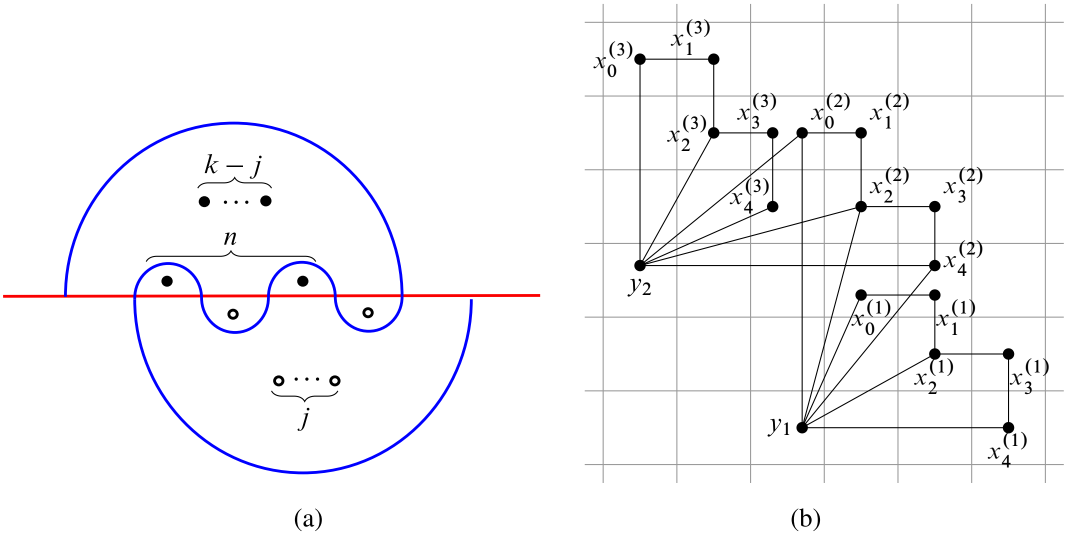

Figure 14: On the left, the block $H(n+j)$ with $1 \le j \le k-1$. On the right, the complex $C_{2,4}$.

staircase, and for each $0 \le i \le n$ the generator $x_{2i}^{(j)}$ has a differential to y_j and y_{j-1} (taking $y_0 = y_{k-1} = 0$). The filtration shifts can be readily computed by counting the number of basepoints in the bigons. □

The following proposition describes the knot Floer complex $\mathrm{CFK}^\infty(S^3, K^+_{n,n+k})$ for $n > 0$, $k \ge 0$. The $k = 1$ case of Proposition 4.27 is the content of [8, Thoerem 3.3.14], which in turn implies Theorem 1.3. (To be precise, [8, Thoerem 3.3.14] describes the mirror of $K^+_{n,n+1}$.)

We recall that $K^+_{n_1,n_2} = K^+([2n_1, 1, 2n_2])$, $C_n \cong \mathrm{CFK}^\infty(S^3, T_{2,2n+1})$, the complexes D_s are defined in Definition 4.20 and the complexes $C_{n,k}$ in Definition 4.25.

Proposition 4.27 *For integers $n > 0$, $k \ge 0$, up to homotopy equivalence the knot Floer complex $\mathrm{CFK}^\infty(S^3, K^+_{n,n+k})$ is given by the following.*

- *When $k = 0$,*
$$\mathrm{CFK}^\infty(S^3, K^+_{n,n}) \cong C_n \oplus 2\Big(\bigoplus_{s=1}^{n-1} D_s\Big).$$
- *When $k = 1$,*
$$\mathrm{CFK}^\infty(S^3, K^+_{n,n+1}) \cong C_n \oplus D_n \oplus 2\Big(\bigoplus_{s=1}^{n-1} D_s\Big).$$
- *When $k = 2$,*
$$\mathrm{CFK}^\infty(S^3, K^+_{n,n+2}) \cong C_n \oplus 2\Big(\bigoplus_{s=1}^{n} D_s\Big).$$
- *When $k \ge 2$,*
$$\mathrm{CFK}^\infty(S^3, K^+_{n,n+k}) \cong C_{n,k} \oplus 2\Big(\bigoplus_{s=1}^{n} D_s\Big).$$

Moreover, there exists a choice of basis, such that when $k = 0$, for each $1 \le s \le n-1$ both D_s are supported in filtration level $(f_{n,s}, f_{n,s})$. When $k > 0$, for $1 \le s \le n$, each pair of D_s is supported in filtration levels

$$(f_{n,s}, f_{n,s}) + \left(\frac{(k-1)(k-2)}{2}, -(n-s+1)k+1\right),$$
$$(f_{n,s}, f_{n,s}) + \left(-(n-s+1)k+1, \frac{(k-1)(k-2)}{2}\right),$$

respectively, except for when $k = 1$ the single copy of D_n is supported in $(0,0)$, where

$$f_{n,s} = -\frac{(n-s)(n-s-1)}{2}. \tag{42}$$

Under this basis, each summand D_s is supported in Maslov grading -1; each 0-graded generator has one $-$ marking and each $+1$-graded generator has one $+$ marking.

Proof The statements regarding the homotopy equivalence type of $\mathrm{CFK}^\infty(S^3, K^+_{n,n+k})$ follow from Proposition 4.24, Lemma 4.26 and the discussion between. We are left with the statements regarding the Maslov grading, the marked basis and the filtration levels, which can be proved by examining the process of splitting off D_s summands more closely.

Since we have that for $s \le n$,

$$\Delta_{\mathcal{I},\mathcal{J}}(x^{(s)}_{2i}, y_{s-1}) = (i, s+1-i) + (n-s, n+k-s), \quad \Delta_{\mathcal{I},\mathcal{J}}(x^{(s)}_{2i}, y_s) = (i, s+1-i),$$

the filtration shift from y_s to y_{s-1} (which supports D_s and D_{s-1}, respectively) is

$$-(n-s, n+k-s), \quad s \le n. \tag{43}$$

For a fixed basis B of a complex C, we say B is supported in the filtration level (a,b) if the generator with the lowest i (resp. j) filtration in B is in filtration level a (resp. b).

When $k = 0$, fix a basis such that the summand C_n is supported in filtration level $(0,0)$. By (39) both copies of D_{n-1} are supported in $(0,0)$. By (43), for $1 \le s \le n-1$ the copy of D_s that comes from $H(s)$ is supported in filtration

$$\left(-\sum_{\ell=0}^{n-s-1} \ell, -\sum_{\ell=0}^{n-s-1} \ell\right) = (f_{n,s}, f_{n,s}).$$

The filtration levels of the remaining complex follows from the symmetry of the knot Floer complex. When $k = 1$, fix a basis such that the single copy of D_n is supported in $(0,0)$. (The summand C_n is supported in $(0,0)$ as well.) The filtration levels in this case follows in the exact same way as above.

When $k \ge 2$, fix a basis such that the summand $C_{n,k}$ is supported in filtration level $(0,0)$. It is straightforward to check that $x^{(1)}_0$ is supported in the filtration level

$$\left(\sum_{\ell=1}^{k-2} \ell, n\right) = \left(\frac{(k-1)(k-2)}{2}, n\right).$$

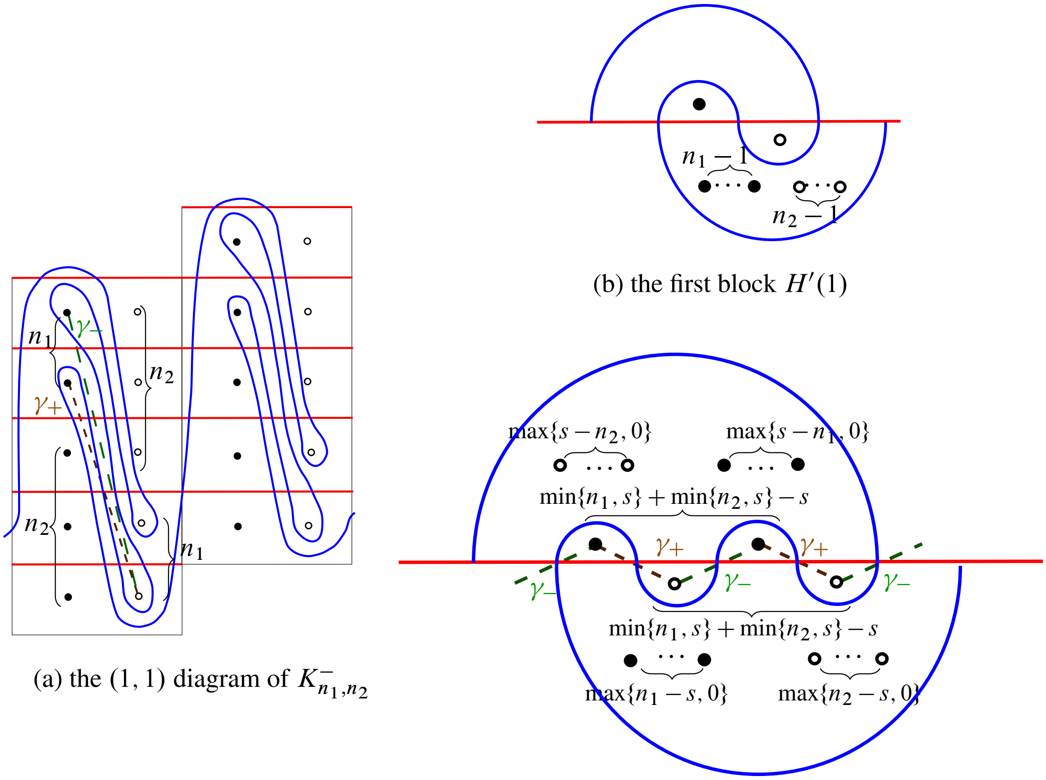

(a) the $(1,1)$ diagram of $K^-_{n_1,n_2}$

(b) the first block $H'(1)$

(c) the s-th block $H'(s)$ with $1 \le s \le n_1+n_2-1$

Figure 15: Illustrations of blocks $H'(s)$.

Then by (39) the copy of D_n that comes from $H(n)$ is supported in $\left(\frac{(k-1)(k-2)}{2}, -k+1\right)$. The filtration levels of the remaining complex follows in the same way as above.

For the statement regarding the Maslov grading, observe (for example, from Figure 13) that every y_s generator in some $H(s)$ is supported in the same Maslov grading t, and every $x_0^{(s)}$ generator in some $H(s)$ is supported in the same Maslov grading $t+1$. On the other hand, the homogeneous element $\sum_s x_0^{(s)}$ is a generator of $H_*(\mathrm{CFK}^\infty(S^3, K^+_{n,n+k})) \cong HF^\infty(S^3)$ and therefore is supported in Maslov grading 0. It follows that $t=-1$. The statement regarding the marked basis can be readily read off by Figure 12(c), using Definition 4.8. □

4.5 Case $K^-([2n_1,1,2n_2])$ with $n_1,n_2>0$

Similarly let us write $K^-_{n_1,n_2}$ for the knot $K^-([2n_1,1,2n_2])$. We still consider the action $\tau^{2n_2}\sigma\tau^{2n_1}$ on the $(1,1)$ diagram, with the difference being the starting slope is $+1$. The resulting $(1,1)$ diagram is depicted in Figure 15(a). Compare with the final diagram in Figure 11. The process for determining $\mathrm{CFK}^\infty(S^3, K^-_{n_1,n_2})$ is almost identical to the process described in the previous section, so we will only include the key steps, being much less elaborate.

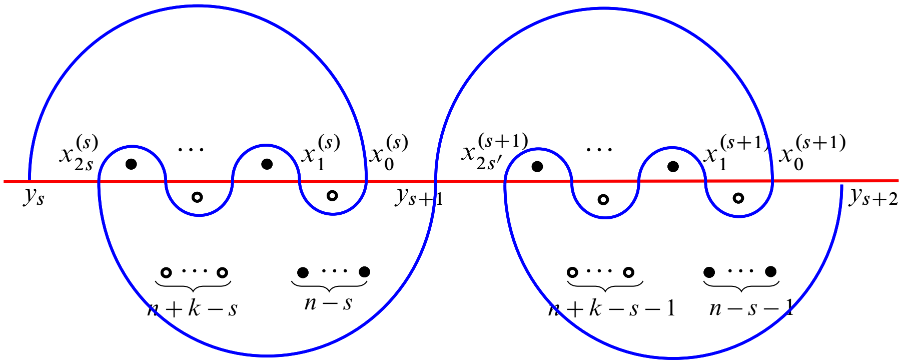

Figure 16: Two consecutive blocks $H'(s)$ (left) and $H'(s+1)$ (right) in $G'(s)$ for $1 \le s \le n$. There is either one basepoint or one of each kind in the upper half plane of $H'(n+1)$ when $s=n$.

To start, we can similarly define the s-th block $H'(s)$ for $1 \le s \le n_1+n_2-1$; we also define the chain complex $G'(1) = \mathrm{CFK}^\infty(S^3, K^-_{n_1,n_2})$, and $G'(i+1) = G'(i)/(\widetilde{H}'(i) \cup \widetilde{H}'(n_1+n_2-i))$, where $\widetilde{H}'(i) = H'(i) \setminus \{\text{right end point}\}$ and $\widetilde{H}'(n_1+n_2-i) = H'(n_1+n_2-i) \setminus \{\text{left end point}\}$ for $1 \le i \le \left\lfloor \frac{n_1+n_2-1}{2} \right\rfloor$. We add the apostrophe to differentiate from the complexes defined in the previous section.

Lemma 4.28 *For $1 \le s \le n_1+n_2-1$, each block $H'(s)$ corresponds to the diagram depicted in Figure 15(c).*

Again due to (30), we have $K^-_{n_1,n_2} = K^-_{n_2,n_1}$. Therefore from now on we only consider knots of the form $K^-_{n,n+k}$ with $n>0$, $k \ge 0$. Similarly as before, we split off D_s summands iteratively until we obtain a small complex. This process in the case of $K^-_{n,n+k}$ is somewhat more straightforward than that in the previous section. We depicted the two consecutive blocks in Figure 16, but in fact we need only to consider the first block $H'(s)$.

Lemma 4.29 *For $n>0$, $k \ge 0$,*

$$\mathrm{CFK}^\infty(S^3, K^-_{n,n+k}) \cong \begin{cases} G(n-1) \oplus 2\left(\bigoplus_{s=1}^{n-1} D_s\right) & \text{if } k=0, \\ G(n) \oplus 2\left(\bigoplus_{s=1}^{n} D_s\right) & \text{if } k \ge 1. \end{cases}$$

Proof For $1 \le s \le n$, label the generators in $H'(s)$ from left to right by $y_s, x_{2s}^{(s)}, \dots, x_0^{(s)}, y_{s+1}$ where $y_{s+1} = H'(s) \cap H'(s+1)$. The differentials are

$$\begin{aligned} \partial x_{2i+1}^{(s)} &= x_{2i}^{(s)} + x_{2i+2}^{(s)}, & 0 \le i \le s-1, \\ \partial x_{2i}^{(s)} &= y_s + y_{s+1}, & 0 \le i \le s, \end{aligned}$$

with filtration shifts

$$\Delta_{\mathcal{I},\mathcal{J}}(x_{2i}^{(s)}, y_s) = (i, s-i),$$
$$\Delta_{\mathcal{I},\mathcal{J}}(x_{2i}^{(s)}, y_{s+1}) = (i, s-i) + (n+k-s, n-s)$$

for $0 \le i \le s$. Therefore performing the filtered change of basis

$$y_s \mapsto y_s + y_{s+1}$$

splits off $\widetilde{H}'(s) = H'(s) \setminus \{y_{s+1}\} \cong D_s$ as a summand. We can split off $\widetilde{H}'(s)$ and $\widetilde{H}'(2n+k-s)$ for $1 \le s \le n-1$ at the same time since $\widetilde{H}'(s) \cap \widetilde{H}'(2n+k-s) = \varnothing$. Due to the symmetry of the knot Floer complex, $\widetilde{H}'(2n+k-s) \cong D_s$. When $k \ge 1$, we can further split off $\widetilde{H}'(n) \cup \widetilde{H}'(n+k) \cong 2D_n$. $\square$

Before stating the theorem, we first clarify some notation. Recall that C_0 is the complex generated by one element and the complexes D_s are defined in Definition 4.20.

Definition 4.30 For $n > 0$, $k \ge 2$, let $C'_{n,k}$ be the complex generated by

$$\{x_i^{(j)} \mid 1 \le j \le k-1,\ 0 \le i \le 2n\} \cup \{y_j \mid 1 \le j \le k\}$$

with differentials

$$\begin{aligned} \partial x_{2i+1}^{(j)} &= x_{2i}^{(j)} + x_{2i+2}^{(j)}, & 0 \le i \le n-1, \\ \partial x_{2i}^{(j)} &= y_j + y_{j+1}, & 0 \le i \le n, \end{aligned}$$

with the filtration shifts

$$\begin{aligned} \Delta_{\mathcal{I},\mathcal{J}}(x_{2i+1}^{(j)}, x_{2i}^{(j)}) &= (1,0), & \\ \Delta_{\mathcal{I},\mathcal{J}}(x_{2i+1}^{(j)}, x_{2i+2}^{(j)}) &= (0,1), & 0 \le i \le n-1, \\ \Delta_{\mathcal{I},\mathcal{J}}(x_{2i}^{(j)}, y_j) &= (i, n-i+j), & \\ \Delta_{\mathcal{I},\mathcal{J}}(x_{2i}^{(j)}, y_{j+1}) &= (i+k-j, n-i), & 0 \le i \le n. \end{aligned}$$

The complex $C'_{1,3}$ is shown below as an example:

$$\begin{tikzcd}
 & x_0^{(2)} \arrow[dl] \arrow[ddd, "3"] & x_1^{(2)} \arrow[l] \arrow[d] & & \\
y_3 & & x_2^{(2)} \arrow[ll] \arrow[ddl] & & \\
 & & & x_0^{(1)} \arrow[dll] \arrow[dd] & x_1^{(1)} \arrow[l] \arrow[d] \\
 & y_2 & & & x_2^{(1)} \arrow[lll, "3"] \arrow[dl] \\
 & & & y_1 &
\end{tikzcd}$$

Proposition 4.31 *For integers $n > 0$, $k \geq 0$, up to homotopy equivalence the knot Floer complex* $\mathrm{CFK}^\infty(S^3, K^-_{n,n+k})$ *is given by the following.*

- *When* $k = 0$,
$$\mathrm{CFK}^\infty(S^3, K^+_{n,n}) \cong C_0 \oplus D_n \oplus 2\left(\bigoplus_{s=1}^{n-1} D_s\right).$$
- *When* $k = 1$,
$$\mathrm{CFK}^\infty(S^3, K^+_{n,n+1}) \cong C_0 \oplus 2\left(\bigoplus_{s=1}^{n} D_s\right).$$
- *When* $k \geq 2$,
$$\mathrm{CFK}^\infty(S^3, K^+_{n,n+k}) \cong C'_{n,k} \oplus 2\left(\bigoplus_{s=1}^{n} D_s\right).$$

Moreover, there exists a choice of basis, such that C_0 is always supported in the filtration level $(0,0)$ and each pair of D_s for $1 \leq s \leq n$ is supported in filtration levels
$$\left(\left(\frac{k+1}{2} + n - s\right)k + \frac{(n-s)(n-s+1)}{2}, \frac{(n-s)(n-s+1)}{2}\right),$$
$$\left(\frac{(n-s)(n-s+1)}{2}, \frac{(n-s)(n-s+1)}{2} + \left(\frac{k+1}{2} + n - s\right)k\right),$$
respectively. Under this basis, each C_0 and D_s summand are supported in Maslov grading 0; each $+1$-graded generator has one $-$ marking and each $+2$-graded generator has one $+$ marking.

Proof From the proof of Lemma 4.29 we see that y_s and y_{s+1} have a filtration difference of

$$(n+k-s, n-s) \quad \text{for } 1 \leq s \leq n. \tag{44}$$

Each D_s is supported by y_s for $1 \leq s \leq n$. For the first two cases, fix a basis such that C_0 is supported in $(0,0)$. For the last case, fix a basis such that $C'_{n,k}$ is supported in $(0,0)$, and then it is straightforward to check that $y_1 \in C'_{n,k}$ has filtration level $((k-1)k/2, 0)$. By (44) we can determine the support of all the D_s that come from $\widetilde{H}'(s)$ for $1 \leq s \leq n$. The filtration levels of the remaining complex follows from the symmetry of the knot Floer complex.

Each y_s generator has the same Maslov grading t, for some integer i, each $x^{(s)}_{2i}$ generator has the same Maslov grading $t+1$ and each $x^{(s)}_{2i+1}$ generator has the same Maslov grading $t+2$. Since the homology is supported in some y_s, we have $t = 0$. The statement regarding the marked basis can be read off from Figure 15(c). □

4.6 Case $K^+([2n_1, 1, -2n_2])$ with $n_1 > 0$, $n_2 > 1$

For suitable orientations of $\widetilde{\alpha}$ and $\widetilde{\beta}$ curve in the $(1,1)$ diagram, the induced orientation for each bigon is the same. See, for example, Figures 17 and 18. By [7, Theorem 1.2], $K^+([2n_1, 1, -2n_2])$ is a (negative)

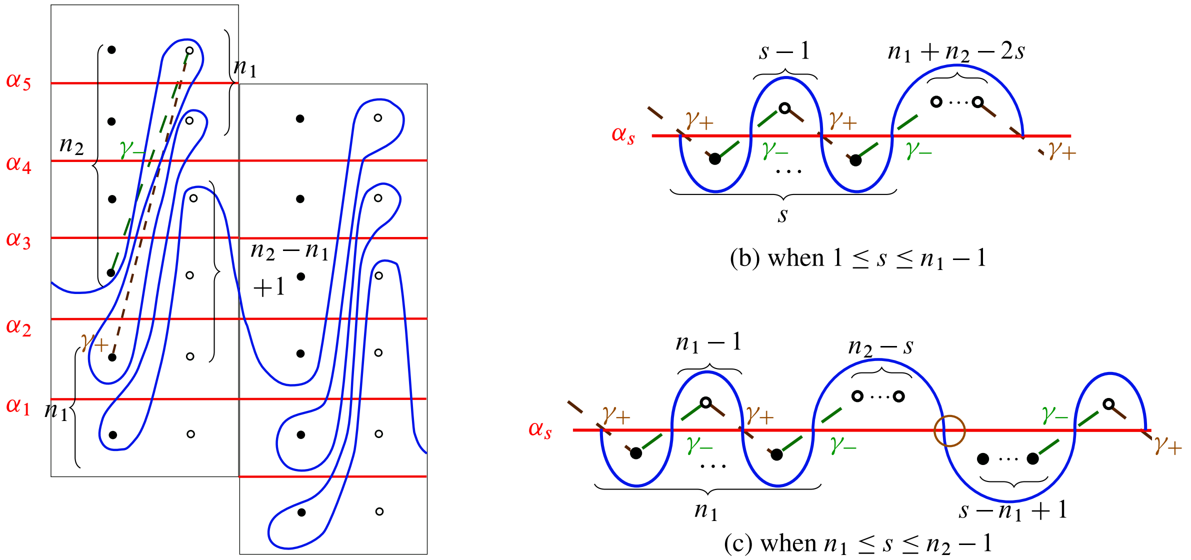

(a) the $(1,1)$ diagram when $n_1=2, n_2=4$

(b) when $1 \le s \le n_1-1$

(c) when $n_1 \le s \le n_2-1$

Figure 17: The case $n_2 \ge n_1$. The only generators without a marking are given by the circled intersection point in (c).

$(1,1)$ L-space knot. Therefore in order to pin down its knot Floer complex, it suffices to record the length of (say) horizontal arrows.

4.6.1 When $n_2 \ge n_1$ The $(1,1)$ diagram in this case is depicted in Figure 17. We proceed as before. For a fixed lift $\tilde{\beta}$, label all the lifts of α which intersect $\tilde{\beta}$ by $\alpha_1,\dots,\alpha_{n_1+n_2-1}$. Identify $\tilde{\alpha}$ with α_s for $1 \le s \le n_1+n_2-1$ in the s-th block. There is an ambiguity in defining the end point of each block. We define the end point of each block to be the first intersection point after $\tilde{\beta}$ travels above a w basepoint in the next block. See the right-hand side of Figure 17.

By Definition 4.6, the slope of γ_+ is n_2 and the slope of γ_- is $-(-n_2+1)=n_2-1$. Observe also that aside from the intersection point circled in Figure 17(c), every intersection point is marked exactly once, where the sign of the marking depends on the parity of the Maslov grading.

We simply count the number of basepoints in the bigons in the upper half plane. This is given by

$$\overbrace{1,\dots,1}^{s-1}, n_1+n_2-2s \quad \text{for } 1 \le s \le n_1-1 \qquad \text{and} \qquad \overbrace{1,\dots,1}^{n_1-1}, n_2-s, 1 \quad \text{for } n_1 \le s \le n_2-1.$$

When $n_1 \ne n_2$, we have $n_2-1 > (n_1+n_2-1)/2$, therefore by the symmetry we can fill out the remaining complex. Specifically, the horizontal-vertical arrows of length $(n_2-n_1,1)$ in the (n_1)-th block is identified after reflection with the horizontal-vertical arrows of length $(1,n_2-n_1)$ in the (n_2-1)-th block. It follows that the remaining horizontal arrows are all of length 1, and there are in total

$$\left(\sum_{i=1}^{n_1} i\right) - 1 = \frac{(n_1+2)(n_1-1)}{2}$$

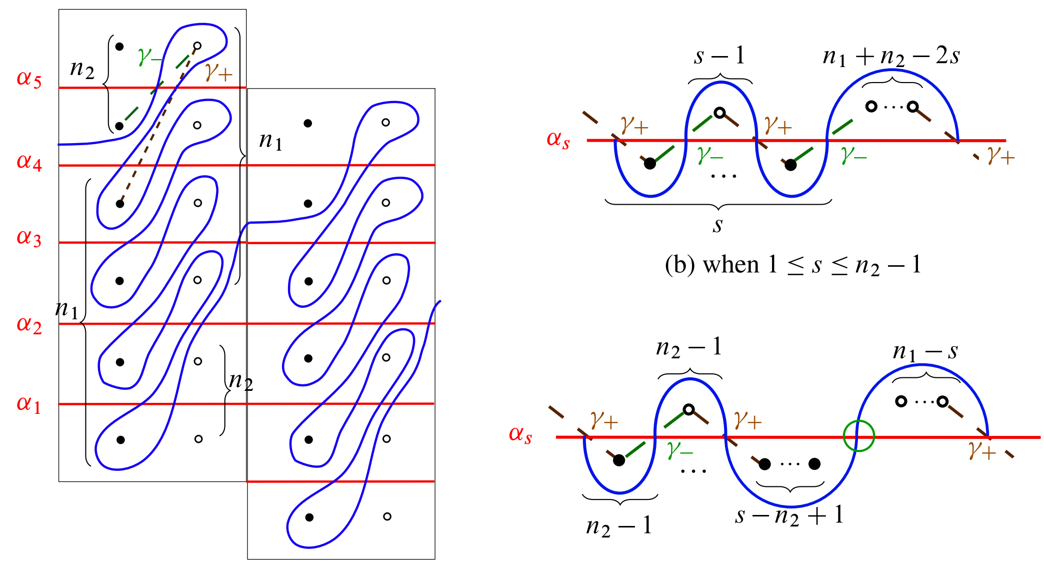

(a) the $(1,1)$ diagram when $n_1=4$, $n_2=2$

(b) when $1 \le s \le n_2-1$

(c) when $n_2 \le s \le n_1-1$

Figure 18: The case $n_2 < n_1$. The only generators without a marking are given by the intersection point circled in (c).

of them. In summary, we have shown that the sequence of lengths of horizontal arrows in the knot Floer complex is given by

$$\underbrace{\overbrace{1,\dots,1}^{s-1}, n_1+n_2-2s,}_{\text{for } 1\le s\le n_1-1} \underbrace{\overbrace{1,\dots,1}^{n_1-1}, n_2-s, 1,}_{\text{for } n_1\le s\le n_2-1} \overbrace{1,\dots,1}^{\frac{(n_1+2)(n_1-1)}{2}}.$$

Moreover, the only generators without a marking are those whose outgoing horizontal arrows are of length n_2-s in the s-th block for $n_1 \le s \le n_2-1$. The above analysis does not cover the case when $n_1=n_2$, but it is straightforward to check that the conclusion also holds there. (When $n_1=n_2$, the (n_1)-th block consists of n_1-1 bigons in each half plane, where each bigon has exactly one basepoint, and the rest of the complex follows from symmetry.)

4.6.2 When $n_2 < n_1$ The $(1,1)$ diagram in this case is depicted in Figure 18. This case is parallel to the previous case, and one can similarly work out the sequence of length of horizontal arrows using the right-hand side diagrams in Figure 18. Putting together the discussion on both cases, we have proved the following.

Proposition 4.32 *For $n_1>0$, $n_2>1$, $K^+([2n_1,1,-2n_2])$ is a negative L-space knot, with the length of horizontal arrows given in order by the follows.*

- *When $n_2 \ge n_1$,*

$$\underbrace{\overbrace{1,\dots,1}^{s-1}, n_1+n_2-2s,}_{\text{for } 1\le s\le n_1-1} \underbrace{\overbrace{1,\dots,1}^{n_1-1}, \overline{n_2-s}, 1,}_{\text{for } n_1\le s\le n_2-1} \overbrace{1,\dots,1}^{\frac{(n_1+2)(n_1-1)}{2}}.$$

Given a basis, each generator with odd Maslov grading has one $-$ marking. Each generator whose outgoing horizontal arrow is marked by the overline has no marking. Apart from them, each generator with even Maslov grading has one $+$ marking.

- *When* $n_2 < n_1$,

$$\underbrace{\overbrace{1,\dots,1}^{s-1}, n_1+n_2-2s}_{\text{for } 1\le s\le n_2-1}, \underbrace{\overbrace{1,\dots,1}^{n_2-1}, \overline{n_1-s}}_{\text{for } n_2\le s\le n_1-1}, \overbrace{1,\dots,1}^{\frac{(n_2+2)(n_2-1)}{2}}.$$

Given a basis, each generator whose incoming horizontal arrow is marked by the overline has no marking. Apart from them, each generator with odd Maslov grading has one $-$ marking. Each generator with even Maslov grading has one $+$ marking.

4.7 Case $K^-([2n_1, 1, -2n_2])$ with $n_1 > 0, n_2 > 1$

By [7, Theorem 1.2], $K^-([2n_1, 1, -2n_2])$ is a positive $(1,1)$ L-space knot. It suffices to record (say) the length of vertical arrows. The process to determine such a sequence is entirely parallel to the process in Section 4.6. Therefore we will skip the proof, giving only the conclusion, as follows.

Proposition 4.33 *For* $n_1 > 0, n_2 > 1$, $K^-([2n_1, 1, -2n_2])$ *is a positive L-space knot, with the length of vertical arrows given in order by the follows.*

- *When* $n_2 \ge n_1 + 2$,

$$\underbrace{\overbrace{1,\dots,1}^{s-1}, n_1+n_2-2s}_{\text{for } 1\le s\le n_1}, \underbrace{\overbrace{1,\dots,1}^{n_1}, \overline{n_2-s-1}}_{\text{for } n_1+1\le s\le n_2-2}, \overbrace{1,\dots,1}^{\frac{n_1(n_1+3)}{2}}.$$

Given a basis, each generator with even Maslov grading has one $-$ marking. Each generator whose outgoing vertical arrow is marked by the overline has no marking. Apart from them, each generator with odd Maslov grading has one $+$ marking.

- *When* $n_2 \le n_1 + 1$,

$$\underbrace{\overbrace{1,\dots,1}^{s-1}, n_1+n_2-2s}_{\text{for } 1\le s\le n_2-2}, \overbrace{1,\dots,1}^{n_2-2}, \overline{n_1-n_2+1}, \underbrace{\overbrace{1,\dots,1}^{n_2-1}, \overline{n_1-s+1}}_{\text{for } n_2\le s\le n_1}, \overbrace{1,\dots,1}^{\frac{n_2(n_2-1)}{2}}.$$

Given a basis, each generator whose incoming vertical arrow is marked by the overline has no marking. Apart from them, each generator with even Maslov grading has one $-$ marking. Each generator with odd Maslov grading has one $+$ marking.

Acknowledgements

I would like to thank my advisor Jen Hom for encouragement and support. I am grateful to Adam Levine, Fraser Binns and Tye Lidman for helpful conversations. I also want to express my appreciation for the amazing thesis [8] by Jonathan Hales. I thank an anonymous referee for helpful suggestions.

References

[1] **S Akbulut**, *A solution to a conjecture of Zeeman*, Topology 30:3 (1991) 513–515 MR

[2] **S Akbulut**, **Ç Karakurt**, *Heegaard Floer homology of some Mazur type manifolds*, Proc. Amer. Math. Soc. 142:11 (2014) 4001–4013 MR

[3] **S Akbulut**, **R Kirby**, *Mazur manifolds*, Michigan Math. J. 26:3 (1979) 259–284 MR

[4] **F Binns**, **H Zhou**, $(1,1)$ *almost L-space knots*, Indiana Univ. Math. J. 74:5 (2025) 1257–1291 MR

[5] **I Dai**, **J Hom**, **M Stoffregen**, **L Truong**, *More concordance homomorphisms from knot Floer homology*, Geom. Topol. 25:1 (2021) 275–338 MR

[6] **I Dai**, **J Hom**, **M Stoffregen**, **L Truong**, *Homology concordance and knot Floer homology*, Math. Ann. 390:4 (2024) 6111–6186 MR

[7] **J E Greene**, **S Lewallen**, **F Vafaee**, $(1,1)$ *L-space knots*, Compos. Math. 154:5 (2018) 918–933 MR

[8] **J Hales**, *Exotic four-manifolds, corks, and Heegaard Floer homology*, PhD thesis, State University of New York at Stony Brook (2013) MR Available at https://www.proquest.com/docview/1432009810

[9] **J Hanselman**, **L Watson**, *Cabling in terms of immersed curves*, Geom. Topol. 27:3 (2023) 925–952 MR

[10] **M Hedden**, **A S Levine**, *A surgery formula for knot Floer homology*, Quantum Topol. 15:2 (2024) 229–336 MR

[11] **J Hom**, **A S Levine**, **T Lidman**, *Knot concordance in homology cobordisms*, Duke Math. J. 171:15 (2022) 3089–3131 MR

[12] **L H Kauffman**, **S Lambropoulou**, *Classifying and applying rational knots and rational tangles*, from "Physical knots: knotting, linking, and folding geometric objects in $\mathbb{R}^3$" (Las Vegas, NV, 2001) (J A Calvo, K C Millett, E J Rawdon, editors), Contemp. Math. 304, Amer. Math. Soc., Providence, RI (2002) 223–259 MR

[13] **A S Levine**, *Nonsurjective satellite operators and piecewise-linear concordance*, Forum Math. Sigma 4 (2016) art. id. e34 MR

[14] **R Lipshitz**, **P S Ozsvath**, **D P Thurston**, *Bordered Heegaard Floer homology*, Mem. Amer. Math. Soc. 1216, Amer. Math. Soc., Providence, RI (2018) MR

[15] **P Ozsváth**, **Z Szabó**, *Heegaard Floer homology and alternating knots*, Geom. Topol. 7 (2003) 225–254 MR

[16] **P Ozsváth**, **Z Szabó**, *Holomorphic disks and knot invariants*, Adv. Math. 186:1 (2004) 58–116 MR

[17] **P Ozsváth**, **Z Szabó**, *On knot Floer homology and lens space surgeries*, Topology 44:6 (2005) 1281–1300 MR

[18] **I Petkova**, *Cables of thin knots and bordered Heegaard Floer homology*, Quantum Topol. 4:4 (2013) 377–409 MR

[19] **L Truong**, *A refinement of the Ozsváth–Szabó large integer surgery formula and knot concordance*, Proc. Amer. Math. Soc. 149:4 (2021) 1757–1771 MR

[20] **H Zhou**, *Homology concordance and an infinite rank free subgroup*, J. Topol. 14:4 (2021) 1369–1395 MR

[21] **H Zhou**, *A filtered mapping cone formula for cables of the knot meridian* (2022) arXiv 2208.11289

HUGO ZHOU hugozhou@umich.edu

Department of Mathematics, University of Michigan, Ann Arbor, MI, United States

Received: July 21, 2023 Revised: October 19, 2024

ALGEBRAIC & GEOMETRIC TOPOLOGY

msp.org/agt

See inside back cover or msp.org/agt for submission instructions.

The subscription price for 2026 is US $795/year for the electronic version, and $1170/year (+$80, if shipping outside the US) for print and electronic. Subscriptions, requests for back issues and changes of subscriber address should be sent to MSP. Algebraic & Geometric Topology is indexed by Mathematical Reviews, Zentralblatt MATH, Current Mathematical Publications and the Science Citation Index.

Algebraic & Geometric Topology (ISSN 1472-2747 printed, 1472-2739 electronic) is published 9 times per year and continuously online, by Mathematical Sciences Publishers, 2000 Allston Way # 59, Berkeley, CA 94701-4004. Periodical rate postage paid at Oakland, CA 94615-9651, and additional mailing offices. POSTMASTER: send address changes to Mathematical Sciences Publishers, 2000 Allston Way # 59, Berkeley, CA 94701-4004.

AGT peer review and production are managed by EditFlow® from MSP.

PUBLISHED BY

mathematical sciences publishers

nonprofit scientific publishing

https://msp.org/

ALGEBRAIC & GEOMETRIC TOPOLOGY

Volume 26 Issue 5 (pages 1597–1963) 2026